

Robust high-order low-rank BUG integrators based on explicit Runge-Kutta methods

Fabio Nobile¹ and Sébastien Riffaud^{1*}

¹CSQI Chair, École Polytechnique Fédérale de Lausanne, 1015
Lausanne, Switzerland.

*Corresponding author(s). E-mail(s): sebastien.riffaud@epfl.ch;

Abstract

In this work, we propose high-order basis-update & Galerkin (BUG) integrators based on explicit Runge-Kutta methods for large-scale matrix differential equations. These dynamical low-rank integrators are high-order extensions of the BUG integrator [1] and are constructed by performing a BUG step at each stage of the Runge-Kutta method. In this way, the resulting Runge-Kutta BUG integrator is robust to the presence of small singular values and does not involve backward time-integration steps. We provide an error bound, which shows that the Runge-Kutta BUG integrator retains the order of convergence of the associated Runge-Kutta method until the error reaches a plateau corresponding to the low-rank truncation error and which vanishes as the rank becomes full. This error bound is finally validated experimentally on three numerical test cases. The results demonstrate the high-order convergence of the Runge-Kutta BUG integrator and its superior accuracy compared to other dynamical low-rank integrators proposed in the literature.

Keywords: Dynamical low-rank approximation, Matrix differential equations, Basis-Update & Galerkin integrators, Runge-Kutta methods

1 Introduction

Dynamical low-rank approximations (DLRAs) enable a significant reduction in the computational cost associated with numerical integration of large-scale matrix differential equations:

$$\dot{\mathbf{A}} = \mathbf{F}(t, \mathbf{A}), \quad \mathbf{A}(0) = \mathbf{A}_0 \in \mathbb{R}^{n \times m}, \quad (1)$$

which appear in many applications, such as kinetic equations [2–8] due to the large phase space, stochastic simulations [9–17] due to the repeated evaluation of the solution for different realizations of the random terms, or sequential parameter estimation [18–21] when tracking solutions for several parameter values. The main idea of DLRAs consists in approximating the solution \mathbf{A} by a low-rank matrix \mathbf{Y} in an SVD-like form:

$$\mathbf{Y}(t) = \mathbf{U}(t)\mathbf{S}(t)\mathbf{V}(t)^T \in \mathbb{R}^{n \times m}, \quad (2)$$

where $\mathbf{U} \in \mathbb{R}^{n \times r}$ and $\mathbf{V} \in \mathbb{R}^{m \times r}$ are orthonormal matrices, $\mathbf{S} \in \mathbb{R}^{r \times r}$ is a square invertible matrix (not necessarily diagonal), and $r \leq \min\{n, m\}$ is the rank of \mathbf{Y} .

A challenging issue concerns the time-integration of the different factors \mathbf{U} , \mathbf{S} , and \mathbf{V} . Perhaps the most intuitive approach is to consider the differential equations, derived in [22], that describe the evolution of the low-rank factorization over time:

$$\begin{cases} \dot{\mathbf{U}} = (\mathbf{I} - \mathbf{U}\mathbf{U}^T) \mathbf{F}(t, \mathbf{Y}) \mathbf{V} \mathbf{S}^{-1} \\ \dot{\mathbf{S}} = \mathbf{U}^T \mathbf{F}(t, \mathbf{Y}) \mathbf{V} \\ \dot{\mathbf{V}} = (\mathbf{I} - \mathbf{V}\mathbf{V}^T) \mathbf{F}(t, \mathbf{Y})^T \mathbf{U} \mathbf{S}^{-T}, \end{cases} \quad (3)$$

where we have assumed that $\mathbf{U}^T \dot{\mathbf{U}} = \mathbf{V}^T \dot{\mathbf{V}} = \mathbf{0}$. Unfortunately, this system involves the inverse of \mathbf{S} , which can cause severe time-step size restrictions if the singular values of \mathbf{S} are small, since the step size of standard time-integration schemes must be proportional to the smallest nonzero singular value. An equivalent formulation to (3) is obtained by projecting the matrix differential equation (1) onto the tangent space of the manifold \mathcal{M}_r of rank- r matrices:

$$\dot{\mathbf{Y}} = \mathcal{P}_{\mathbf{Y}}(\mathbf{F}(t, \mathbf{Y})), \quad \mathbf{Y}(0) = \mathbf{Y}_0 \in \mathcal{M}_r, \quad (4)$$

where

$$\mathcal{P}_{\mathbf{Y}}(\mathbf{X}) = \mathbf{U}\mathbf{U}^T \mathbf{X} - \mathbf{U}\mathbf{U}^T \mathbf{X} \mathbf{V} \mathbf{V}^T + \mathbf{X} \mathbf{V} \mathbf{V}^T \quad (5)$$

stands for the orthogonal projection of $\mathbf{X} \in \mathbb{R}^{n \times m}$ onto the tangent space at $\mathbf{Y} = \mathbf{U}\mathbf{S}\mathbf{V}^T \in \mathcal{M}_r$. In the projection-splitting integrator [23, 24], this tangent-space projection is split into three alternating subprojections using the Lie-Trotter or Strang splitting. The resulting low-rank integrator is robust to the presence of small singular values, but the step associated with the update of \mathbf{S} integrates the solution backward in time, which can lead to instabilities for parabolic and hyperbolic problems [25].

In recent years, several dynamical low-rank integrators that are robust to the presence of small singular values and do not involve backward time-integration steps have been proposed:

- the basis-update & Galerkin (BUG) integrators [1, 26, 27], where \mathbf{U} and \mathbf{V} are first updated using the tangent-space projection, and then \mathbf{S} is updated using a Galerkin projection of the matrix differential equation (1) onto the updated bases \mathbf{U} and \mathbf{V} ;
- the projected Runge-Kutta methods [28, 29], in which the projected differential equation (4) is integrated using a Runge-Kutta method which includes a truncation step that maintains low-rank approximations.

The convergence of the BUG integrator is limited to order one, but recent efforts are made to extend this dynamical low-rank integrator to higher orders. For instance, second-order extensions based on the midpoint rule have been proposed in [30, 31]. On the other hand, projected Runge-Kutta methods have high-order error bounds for time-explicit discretizations. However, these dynamical low-rank integrators do not share the conservation properties [32] offered by the Galerkin projection of the BUG integrator.

In this work, we propose high-order BUG integrators based on explicit Runge-Kutta methods. These dynamical low-rank integrators are high-order extensions of the BUG integrator and are constructed by performing a BUG step at each stage of the Runge-Kutta method. In this way, the resulting dynamical low-rank integrators are robust to the presence of small singular values and do not involve backward time-integration steps. Moreover, compared with projected Runge-Kutta methods, the only difference is that the tangent-space projection is replaced by the Galerkin projection of the BUG integrator. As a result, Runge-Kutta BUG integrators present two advantages. First, conservation properties can be preserved more easily. Second, the Galerkin projection of Runge-Kutta BUG integrators is more accurate than the tangent-space projection of projected Runge-Kutta methods for approximating \mathbf{F} at the discrete level (see Proposition 3). Furthermore, we prove in Theorem 2 that the Runge-Kutta BUG integrator retains the order of convergence of the associated Runge-Kutta method until the error reaches a plateau corresponding to the low-rank truncation error and which vanishes as the rank becomes full. In particular, this property holds for any explicit Runge-Kutta method, allowing in practice the construction of various high-order dynamical low-rank integrators.

The remainder of the paper is organized as follows. Section 2 introduces the first-order BUG integrator based on the forward Euler method. In Section 3, we present high-order extensions of the BUG integrator based on explicit Runge-Kutta methods. Then, Section 4 analyzes the convergence of the proposed dynamical low-rank integrators. In Section 5, the resulting error bound is validated experimentally on three numerical test cases. Finally, Section 6 draws some conclusions and perspectives.

2 The BUG integrator based on the forward Euler method

The dynamical low-rank integrator proposed in this work is an extension of the first-order BUG integrator [1]. For the convenience of the reader, we start by presenting the latter in the time-explicit case, i.e. for the forward Euler method. Let the time be discretized using a fixed time-step size $h > 0$. The integration of the rank- r solution $\mathbf{Y}_k = \mathbf{U}_k \mathbf{S}_k \mathbf{V}_k^T$ from time t_k to $t_k + h$ reads:

1. **K-step:** Assemble

$$\mathbf{K} = [\mathbf{U}_k \quad \mathbf{F}(t_k, \mathbf{Y}_k) \mathbf{V}_k] \in \mathbb{R}^{n \times 2r}, \quad (6)$$

and compute $\hat{\mathbf{U}}_{k+1} \in \mathbb{R}^{n \times \hat{r}}$ with $\hat{r} \in \{r, \dots, \min\{n, m, 2r\}\}$ as an orthonormal basis of the range of \mathbf{K} (e.g., by QR decomposition), in short $\hat{\mathbf{U}}_{k+1} = \text{ortho}(\mathbf{K})$.

2. **L-step:** Assemble

$$\mathbf{L} = [\mathbf{V}_k \quad \mathbf{F}(t_k, \mathbf{Y}_k)^T \mathbf{U}_k] \in \mathbb{R}^{m \times 2r}, \quad (7)$$

and compute the augmented basis $\widehat{\mathbf{V}}_{k+1} = \text{ortho}(\mathbf{L}) \in \mathbb{R}^{m \times \widehat{r}}$.

3. **S-step:** Set

$$\widehat{\mathbf{S}}_{k+1} = \widehat{\mathbf{U}}_{k+1}^T (\mathbf{Y}_k + h\mathbf{F}(t_k, \mathbf{Y}_k)) \widehat{\mathbf{V}}_{k+1} \in \mathbb{R}^{\widehat{r} \times \widehat{r}}. \quad (8)$$

4. **Truncation step:** Let the r -truncated singular value decomposition (SVD) of $\widehat{\mathbf{S}}_{k+1}$ be $\widehat{\mathbf{S}}_{k+1} = \widehat{\mathbf{\Phi}} \mathbf{\Sigma} \widehat{\mathbf{\Psi}}^T$, where $\widehat{\mathbf{\Phi}}, \widehat{\mathbf{\Psi}} \in \mathbb{R}^{\widehat{r} \times r}$ are orthonormal matrices and $\mathbf{\Sigma} \in \mathbb{R}^{r \times r}$ is a diagonal matrix with non-negative real numbers on the diagonal. Set

$$\begin{aligned} \mathbf{U}_{k+1} &= \widehat{\mathbf{U}}_{k+1} \widehat{\mathbf{\Phi}}, \\ \mathbf{S}_{k+1} &= \mathbf{\Sigma}, \\ \mathbf{V}_{k+1} &= \widehat{\mathbf{V}}_{k+1} \widehat{\mathbf{\Psi}}. \end{aligned} \quad (9)$$

To simplify notation, let $\llbracket \mathbf{X} \rrbracket_r$ denote the projection of \mathbf{X} onto \mathcal{M}_r , which is given by the r -truncated SVD of \mathbf{X} . The BUG integrator based on the forward Euler method is summarized in Algorithm 1. Note that the rank r has been fixed here for simplicity, but an adaptive rank can also be used to truncate the augmented solution $\widehat{\mathbf{Y}}_{k+1} = \widehat{\mathbf{U}}_{k+1} \widehat{\mathbf{S}}_{k+1} \widehat{\mathbf{V}}_{k+1}^T$.

3 Extension of the BUG integrator to high-order explicit Runge-Kutta methods

We now extend the BUG integrator to high-order explicit Runge-Kutta methods. Let us consider the explicit Runge-Kutta method:

$$\begin{aligned} \mathbf{A}_{ki} &= \mathbf{A}_k + h \sum_{j=1}^{i-1} a_{ij} \mathbf{F}(t_{kj}, \mathbf{A}_{kj}), \quad i = 1, \dots, s, \\ \mathbf{A}_{k+1} &= \mathbf{A}_k + h \sum_{i=1}^s b_i \mathbf{F}(t_{ki}, \mathbf{A}_{ki}), \end{aligned} \quad (10)$$

where $t_{ki} = t_k + c_i h$. The main idea is to perform one step of the BUG integrator at each stage of the Runge-Kutta method. To this end, the key point concerns the definition of the augmented bases. Consider, for example, the final stage with the initial value \mathbf{Y}_k :

$$\mathbf{Y}_{k+1} = \mathbf{Y}_k + h \sum_{i=1}^s b_i \mathbf{F}(t_{ki}, \mathbf{Y}_{ki}).$$

The augmented bases $\widehat{\mathbf{U}}_{k+1}$ and $\widehat{\mathbf{V}}_{k+1}$ are constructed here to represent exactly \mathbf{Y}_k and the tangent-space projection of the different terms $\mathbf{F}(t_{ki}, \mathbf{Y}_{ki})$. Notably, \mathbf{Y}_k is represented on the left and right bases \mathbf{U}_k and \mathbf{V}_k , while the tangent-space projection of $\mathbf{F}(t_{ki}, \mathbf{Y}_{ki})$ is represented according to equation (5) on $[\mathbf{U}_{ki} \quad \mathbf{F}_{ki} \mathbf{V}_{ki}]$ and

$[\mathbf{V}_{ki} \ \mathbf{F}_{ki}^T \mathbf{U}_{ki}]$, where $\mathbf{F}_{ki} = \mathbf{F}(t_{ki}, \mathbf{Y}_{ki})$. Moreover, let us introduce the coefficients α_{ij} and β_i , defined as

$$\alpha_{ij} = \begin{cases} 1 & \text{if } a_{ij} \neq 0 \\ 0 & \text{otherwise} \end{cases} \quad \text{and} \quad \beta_i = \begin{cases} 1 & \text{if } b_i \neq 0 \\ 0 & \text{otherwise,} \end{cases}$$

which will allow us to discard the bases that are not involved in the different tangent-space projections. The augmented bases $\widehat{\mathbf{U}}_{k+1}$ and $\widehat{\mathbf{V}}_{k+1}$ are given by

$$\begin{aligned} \widehat{\mathbf{U}}_{k+1} &\leftarrow \text{ortho}([\mathbf{U}_k \ \beta_1 \mathbf{U}_{k1} \ \beta_1 \mathbf{F}_{k1} \mathbf{V}_{k1} \ \cdots \ \beta_s \mathbf{U}_{ks} \ \beta_s \mathbf{F}_{ks} \mathbf{V}_{ks}]), \\ \widehat{\mathbf{V}}_{k+1} &\leftarrow \text{ortho}([\mathbf{V}_k \ \beta_1 \mathbf{V}_{k1} \ \beta_1 \mathbf{F}_{k1}^T \mathbf{U}_{k1} \ \cdots \ \beta_s \mathbf{V}_{ks} \ \beta_s \mathbf{F}_{ks}^T \mathbf{U}_{ks}]), \end{aligned}$$

where the terms $\beta_1 \mathbf{U}_{k1}$ and $\beta_1 \mathbf{V}_{k1}$ can be removed since $\mathbf{U}_{k1} = \mathbf{U}_k$ and $\mathbf{V}_{k1} = \mathbf{V}_k$. The Runge-Kutta BUG integrator associated with the Runge-Kutta method (10) is finally described in Algorithm 2. As mentioned previously, an adaptative rank can also be used to ensure, for example, that the error of the truncation step is smaller than a prescribed tolerance.

Remark 1. *The rank of the augmented solution $\widehat{\mathbf{Y}}_{k+1}$ (resp. $\widehat{\mathbf{Y}}_{k,i+1}$) is at most $2rs$ (resp. $2ri$).*

Remark 2. *When $r = \min\{n, m\}$, the Runge-Kutta BUG integrator is equivalent to the associated Runge-Kutta method, since the manifold \mathcal{M}_r corresponds to the whole Euclidean space $\mathbb{R}^{n \times m}$, and there is therefore no projection or truncation error.*

Algorithm 1 First-order BUG integrator [1] based on the forward Euler method

Input: \mathbf{Y}_0 .

Output: $\mathbf{Y}_1, \dots, \mathbf{Y}_N$.

```

1: for  $k = 0, \dots, N - 1$  do
2:    $\mathbf{Y}_k := \mathbf{U}_k \mathbf{S}_k \mathbf{V}_k^T$ ;
3:    $\mathbf{F}_k \leftarrow \mathbf{F}(t_k, \mathbf{Y}_k)$ ;
4:    $\widehat{\mathbf{U}}_{k+1} \leftarrow \text{ortho}([\mathbf{U}_k \ \mathbf{F}_k \mathbf{V}_k])$ ; ▷ K-step (6)
5:    $\widehat{\mathbf{V}}_{k+1} \leftarrow \text{ortho}([\mathbf{V}_k \ \mathbf{F}_k^T \mathbf{U}_k])$ ; ▷ L-step (8)
6:    $\widehat{\mathbf{S}}_{k+1} \leftarrow \widehat{\mathbf{U}}_{k+1}^T (\mathbf{Y}_k + h \mathbf{F}_k) \widehat{\mathbf{V}}_{k+1}$ ; ▷ S-step (7)
7:    $\widehat{\mathbf{Y}}_{k+1} \leftarrow \widehat{\mathbf{U}}_{k+1} \widehat{\mathbf{S}}_{k+1} \widehat{\mathbf{V}}_{k+1}^T$ ;
8:    $\mathbf{Y}_{k+1} \leftarrow \llbracket \widehat{\mathbf{Y}}_{k+1} \rrbracket_r$ . ▷ Truncation step (9)
9: end

```

Algorithm 2 High-order explicit Runge-Kutta BUG integrator

Input: \mathbf{Y}_0 .

Output: $\mathbf{Y}_1, \dots, \mathbf{Y}_N$.

```

1: for  $k = 0, \dots, N - 1$  do
2:    $\mathbf{Y}_{k1} \leftarrow \mathbf{Y}_k$ ;
3:   for  $i = 1, \dots, s - 1$  do
4:      $\mathbf{Y}_{ki} := \mathbf{U}_{ki} \mathbf{S}_{ki} \mathbf{V}_{ki}^T$ ;
5:      $\mathbf{F}_{ki} \leftarrow \mathbf{F}(t_k + c_i h, \mathbf{Y}_{ki})$ ;
6:      $\widehat{\mathbf{U}}_{k,i+1} \leftarrow \text{ortho}([\mathbf{U}_k \ \alpha_{i+1,1} \mathbf{F}_{k1} \mathbf{V}_{k1} \ \dots \ \alpha_{i+1,i} \mathbf{U}_{ki} \ \alpha_{i+1,i} \mathbf{F}_{ki} \mathbf{V}_{ki}]);$ 
7:      $\widehat{\mathbf{V}}_{k,i+1} \leftarrow \text{ortho}([\mathbf{V}_k \ \alpha_{i+1,1} \mathbf{F}_{k1}^T \mathbf{U}_{k1} \ \dots \ \alpha_{i+1,i} \mathbf{V}_{ki} \ \alpha_{i+1,i} \mathbf{F}_{ki}^T \mathbf{U}_{ki}]);$ 
8:      $\widehat{\mathbf{S}}_{k,i+1} \leftarrow \widehat{\mathbf{U}}_{k,i+1}^T (\mathbf{Y}_k + h(a_{i+1,1} \mathbf{F}_{k1} + \dots + a_{i+1,i} \mathbf{F}_{ki})) \widehat{\mathbf{V}}_{k,i+1}$ ;
9:      $\widehat{\mathbf{Y}}_{k,i+1} \leftarrow \widehat{\mathbf{U}}_{k,i+1} \widehat{\mathbf{S}}_{k,i+1} \widehat{\mathbf{V}}_{k,i+1}^T$ ;
10:     $\mathbf{Y}_{k,i+1} \leftarrow \llbracket \widehat{\mathbf{Y}}_{k,i+1} \rrbracket_r$ ;
11:  end
12:   $\mathbf{Y}_{ks} := \mathbf{U}_{ks} \mathbf{S}_{ks} \mathbf{V}_{ks}^T$ ;
13:   $\mathbf{F}_{ks} \leftarrow \mathbf{F}(t_k + c_s h, \mathbf{Y}_{ks})$ ;
14:   $\widehat{\mathbf{U}}_{k+1} \leftarrow \text{ortho}([\mathbf{U}_k \ \beta_1 \mathbf{F}_{k1} \mathbf{V}_{k1} \ \dots \ \beta_s \mathbf{U}_{ks} \ \beta_s \mathbf{F}_{ks} \mathbf{V}_{ks}]);$ 
15:   $\widehat{\mathbf{V}}_{k+1} \leftarrow \text{ortho}([\mathbf{V}_k \ \beta_1 \mathbf{F}_{k1}^T \mathbf{U}_{k1} \ \dots \ \beta_s \mathbf{V}_{ks} \ \beta_s \mathbf{F}_{ks}^T \mathbf{U}_{ks}]);$ 
16:   $\widehat{\mathbf{S}}_{k+1} \leftarrow \widehat{\mathbf{U}}_{k+1}^T (\mathbf{Y}_k + h(b_1 \mathbf{F}_{k1} + \dots + b_s \mathbf{F}_{ks})) \widehat{\mathbf{V}}_{k+1}$ ;
17:   $\widehat{\mathbf{Y}}_{k+1} \leftarrow \widehat{\mathbf{U}}_{k+1} \widehat{\mathbf{S}}_{k+1} \widehat{\mathbf{V}}_{k+1}^T$ .
18:   $\mathbf{Y}_{k+1} \leftarrow \llbracket \widehat{\mathbf{Y}}_{k+1} \rrbracket_r$ .
19: end

```

4 Convergence analysis

In this section, we analyze the convergence of the Runge-Kutta BUG integrator in the case where the rank r is fixed and for a time-step size h sufficiently small, say $h \leq h_0$ (see Theorem 3.4 of Chapter 2 in [33] for the exact definition of h_0). The present analysis is based on two assumptions. The first assumption implies the existence and uniqueness of the exact solution \mathbf{A} according to the Picard-Lindelöf theorem, while the second assumption is needed in Theorem 3.1 of Chapter 2 in [33] to analyze the local error of high-order Runge-Kutta methods. Furthermore, this analysis is done in the Frobenius norm $\|\cdot\|_F$, and $\langle \cdot, \cdot \rangle_F$ will stand for the Frobenius inner product in the following.

Assumption 1. $\mathbf{F}(t, \mathbf{X})$ is continuous in time and Lipschitz continuous in \mathbf{X} : there exists a Lipschitz constant $L > 0$ (independent of t) such that

$$\|\mathbf{F}(t, \mathbf{X}_1) - \mathbf{F}(t, \mathbf{X}_2)\|_F \leq L \|\mathbf{X}_1 - \mathbf{X}_2\|_F$$

for all $t \in [0, T]$ and $\mathbf{X}_1, \mathbf{X}_2 \in \mathbb{R}^{n \times m}$.

Assumption 2. Let $\Phi_{\mathbf{F}}^t$ denote the exact flow of \mathbf{F} (i.e., the mapping such that $\mathbf{A}(t) = \Phi_{\mathbf{F}}^t(\mathbf{A}_0)$). When considering a Runge-Kutta method of order p , we assume

that the first p derivatives

$$\frac{d^q}{dt^q} \Phi_{\mathbf{F}}^t(\mathbf{X}), \quad 1 \leq q \leq p,$$

exist and are continuous for all $\mathbf{X} \in \mathbb{R}^{n \times m}$.

4.1 Preliminary results

Compared to [1], we do not assume that \mathbf{F} is bounded for all $\mathbf{X} \in \mathbb{R}^{n \times m}$. For this reason, we start by showing that \mathbf{F} is bounded in a neighbourhood of the exact solution \mathbf{Y} , which can be deduced from Assumption 1 and will be sufficient in the following. Additionally, we show that the exact flow $\Phi_{\mathbf{F}}^t$ is Lipschitz continuous, which is a direct consequence of the Lipschitz continuity of \mathbf{F} .

Proposition 1. *Suppose that Assumption 1 holds. The exact solution $\mathbf{Y}(t)$ of the projected differential equation (4) is bounded by*

$$\|\mathbf{Y}(t) - \mathbf{Y}_0\|_F \leq \int_0^t e^{L(t-s)} \|\mathbf{F}(s, \mathbf{Y}_0)\|_F ds \quad (11)$$

for all $t \in [0, T]$.

Proof. Without loss of generality, assume that $\mathbf{Y}(t) \neq \mathbf{Y}_0$ for all $t \in (0, T)$. If $\mathbf{Y}(t) = \mathbf{Y}_0$ for certain times, consider independently the time subintervals where $\mathbf{Y}(t) \neq \mathbf{Y}_0$. Then, we deduce from Assumption 1 the differential inequality

$$\begin{aligned} \|\mathbf{Y}(t) - \mathbf{Y}_0\|_F \frac{d}{dt} \|\mathbf{Y}(t) - \mathbf{Y}_0\|_F &= \frac{1}{2} \frac{d}{dt} \|\mathbf{Y}(t) - \mathbf{Y}_0\|_F^2 \\ &= \langle \mathbf{Y}(t) - \mathbf{Y}_0, \mathcal{P}_{\mathbf{Y}}(\mathbf{F}(t, \mathbf{Y}(t))) \rangle_F \\ &\leq \|\mathbf{Y}(t) - \mathbf{Y}_0\|_F \|\mathcal{P}_{\mathbf{Y}}(\mathbf{F}(t, \mathbf{Y}(t)))\|_F \\ &\leq \|\mathbf{Y}(t) - \mathbf{Y}_0\|_F \|\mathbf{F}(t, \mathbf{Y}(t))\|_F \\ &\leq \|\mathbf{Y}(t) - \mathbf{Y}_0\|_F (\|\mathbf{F}(t, \mathbf{Y}(t)) - \mathbf{F}(t, \mathbf{Y}_0)\|_F + \|\mathbf{F}(t, \mathbf{Y}_0)\|_F) \\ &\leq \|\mathbf{Y}(t) - \mathbf{Y}_0\|_F (L \|\mathbf{Y}(t) - \mathbf{Y}_0\|_F + \|\mathbf{F}(t, \mathbf{Y}_0)\|_F), \end{aligned}$$

which can be rewritten as

$$\frac{d}{dt} \|\mathbf{Y}(t) - \mathbf{Y}_0\|_F \leq L \|\mathbf{Y}(t) - \mathbf{Y}_0\|_F + \|\mathbf{F}(t, \mathbf{Y}_0)\|_F.$$

Finally, according to the Grönwall's inequality, the exact solution $\mathbf{Y}(t)$ verifies

$$\|\mathbf{Y}(t) - \mathbf{Y}_0\|_F \leq \int_0^t e^{L(t-s)} \|\mathbf{F}(s, \mathbf{Y}_0)\|_F ds,$$

which concludes the proof. \square

Lemma 1. *Suppose that Assumption 1 holds. Then, for $h \leq h_0$, the discrete solution \mathbf{Y}_{ki} of the Runge-Kutta BUG integrator is bounded at each stage $i \in \{1, \dots, s\}$ by*

$$\|\mathbf{Y}_{ki} - \mathbf{Y}_0\|_F \leq (1 + K_{i0}h) \|\mathbf{Y}_k - \mathbf{Y}_0\|_F + h \sum_{j=1}^{i-1} K_{ij} \|\mathbf{F}(t_{kj}, \mathbf{Y}_0)\|_F, \quad (12)$$

where the constants $K_{ij} \geq 0$ are independent of h .

Proof. We proceed by induction. For $i = 1$, the statement is trivial with $K_{1j} = 0$ since $\mathbf{Y}_{k1} = \mathbf{Y}_k$. Then, for $i \in \{2, \dots, s\}$, the induction hypothesis yields the desired result:

$$\begin{aligned} \|\mathbf{Y}_{ki} - \mathbf{Y}_0\|_F &= \left\| \left[\widehat{\mathbf{Y}}_{ki} \right]_r - \mathbf{Y}_0 \right\|_F \\ &\leq \left\| \left[\widehat{\mathbf{Y}}_{ki} \right]_r - \widehat{\mathbf{Y}}_{ki} \right\|_F + \left\| \widehat{\mathbf{Y}}_{ki} - \mathbf{Y}_0 \right\|_F \\ &= \min_{\mathbf{X} \in \mathcal{M}_r} \left\| \mathbf{X} - \widehat{\mathbf{Y}}_{ki} \right\|_F + \left\| \widehat{\mathbf{Y}}_{ki} - \mathbf{Y}_0 \right\|_F \\ &\leq \left\| \mathbf{Y}_k - \widehat{\mathbf{Y}}_{ki} \right\|_F + \left\| \widehat{\mathbf{Y}}_{k,i} - \mathbf{Y}_0 \right\|_F \\ &\leq \left\| \mathbf{Y}_k - \mathbf{Y}_0 \right\|_F + 2h \sum_{j=1}^{i-1} |a_{ij}| \left\| \widehat{\mathbf{U}}_{ki} \widehat{\mathbf{U}}_{ki}^T \mathbf{F}(t_{kj}, \mathbf{Y}_{kj}) \widehat{\mathbf{V}}_{ki} \widehat{\mathbf{V}}_{ki}^T \right\|_F \\ &\leq \left\| \mathbf{Y}_k - \mathbf{Y}_0 \right\|_F + 2h \sum_{j=1}^{i-1} |a_{ij}| \left\| \mathbf{F}(t_{kj}, \mathbf{Y}_{kj}) \right\|_F \\ &\leq \left\| \mathbf{Y}_k - \mathbf{Y}_0 \right\|_F + 2h \sum_{j=1}^{i-1} |a_{ij}| \left(\left\| \mathbf{F}(t_{kj}, \mathbf{Y}_{kj}) - \mathbf{F}(t_{kj}, \mathbf{Y}_0) \right\|_F + \left\| \mathbf{F}(t_{kj}, \mathbf{Y}_0) \right\|_F \right) \\ &\leq \left\| \mathbf{Y}_k - \mathbf{Y}_0 \right\|_F + 2h \sum_{j=1}^{i-1} |a_{ij}| \left(L \left\| \mathbf{Y}_{kj} - \mathbf{Y}_0 \right\|_F + \left\| \mathbf{F}(t_{kj}, \mathbf{Y}_0) \right\|_F \right) \\ &\leq \left(1 + 2h \sum_{j=1}^{i-1} |a_{ij}| L (1 + K_{j0}h) \right) \left\| \mathbf{Y}_k - \mathbf{Y}_0 \right\|_F \\ &\quad + 2h \sum_{j=1}^{i-1} |a_{ij}| \left(\left\| \mathbf{F}(t_{kj}, \mathbf{Y}_0) \right\|_F + Lh \sum_{l=1}^{j-1} K_{jl} \left\| \mathbf{F}(t_{kl}, \mathbf{Y}_0) \right\|_F \right) \\ &\leq (1 + K_{i0}h) \left\| \mathbf{Y}_k - \mathbf{Y}_0 \right\|_F + h \sum_{l=1}^{i-1} K_{il} \left\| \mathbf{F}(t_{kl}, \mathbf{Y}_0) \right\|_F, \end{aligned}$$

where

$$\begin{aligned}
K_{i0} &= 2L \sum_{j=1}^{i-1} |a_{ij}| (1 + K_{j0} h_0), \\
K_{il} &= 2|a_{il}| + 2Lh_0 \sum_{j=l+1}^{i-1} |a_{ij}| K_{jl}, \quad l = 1, \dots, i-2, \\
K_{i,i-1} &= 2|a_{i,i-1}|.
\end{aligned}$$

□

Lemma 2. *Suppose that Assumption 1 holds. Then, for $h \leq h_0$, the discrete solution \mathbf{Y}_k of the Runge-Kutta BUG integrator is bounded by*

$$\|\mathbf{Y}_{k+1} - \mathbf{Y}_0\|_F \leq (1 + \tilde{K}_0 h) \|\mathbf{Y}_k - \mathbf{Y}_0\|_F + h \sum_{i=1}^s \tilde{K}_i \|\mathbf{F}(t_{ki}, \mathbf{Y}_0)\|_F, \quad (13)$$

where the constants $\tilde{K}_i > 0$ are independent of h .

Proof. We proceed in the same way as in Lemma 1. For $k+1=0$, the statement is trivial. Then, for $k+1 \geq 1$, Lemma 1 and the induction hypothesis yield the desired result:

$$\begin{aligned}
\|\mathbf{Y}_{k+1} - \mathbf{Y}_0\|_F &\leq \left\| \mathbf{Y}_k - \hat{\mathbf{Y}}_{k+1} \right\|_F + \left\| \hat{\mathbf{Y}}_{k+1} - \mathbf{Y}_0 \right\|_F \\
&\leq \|\mathbf{Y}_k - \mathbf{Y}_0\|_F + 2h \sum_{i=1}^s |b_i| \left\| \hat{\mathbf{U}}_{ks} \hat{\mathbf{U}}_{ks}^T \mathbf{F}(t_{ki}, \mathbf{Y}_{ki}) \hat{\mathbf{V}}_{ks} \hat{\mathbf{V}}_{ks}^T \right\|_F \\
&\leq \|\mathbf{Y}_k - \mathbf{Y}_0\|_F + 2h \sum_{i=1}^s |b_i| \|\mathbf{F}(t_{ki}, \mathbf{Y}_{ki})\|_F \\
&\leq \|\mathbf{Y}_k - \mathbf{Y}_0\|_F + 2h \sum_{i=1}^s |b_i| (\|\mathbf{F}(t_{ki}, \mathbf{Y}_{ki}) - \mathbf{F}(t_{ki}, \mathbf{Y}_0)\|_F + \|\mathbf{F}(t_{ki}, \mathbf{Y}_0)\|_F) \\
&\leq \|\mathbf{Y}_k - \mathbf{Y}_0\|_F + 2h \sum_{i=1}^s |b_i| (L \|\mathbf{Y}_{ki} - \mathbf{Y}_0\|_F + \|\mathbf{F}(t_{ki}, \mathbf{Y}_0)\|_F) \\
&\leq \left(1 + 2h \sum_{i=1}^s |b_i| L (1 + K_{i0} h) \right) \|\mathbf{Y}_k - \mathbf{Y}_0\|_F \\
&\quad + 2h \sum_{i=1}^s |b_i| \left(\|\mathbf{F}(t_{ki}, \mathbf{Y}_0)\|_F + Lh \sum_{j=1}^{i-1} K_{ij} \|\mathbf{F}(t_{kj}, \mathbf{Y}_0)\|_F \right) \\
&\leq (1 + \tilde{K}_0 h) \|\mathbf{Y}_k - \mathbf{Y}_0\|_F + h \sum_{l=1}^s \tilde{K}_l \|\mathbf{F}(t_{kl}, \mathbf{Y}_0)\|_F,
\end{aligned}$$

where

$$\begin{aligned}\tilde{K}_0 &= 2L \sum_{i=1}^s |b_i|(1 + K_{i0}h_0), \\ \tilde{K}_l &= 2|b_l| + 2Lh_0 \sum_{i=l+1}^s |b_i|K_{il}, \quad l = 1, \dots, s-1, \\ \tilde{K}_s &= 2|b_s|.\end{aligned}$$

□

Proposition 2. *Suppose that Assumption 1 holds. Then, for $h \leq h_0$, the discrete solution of the Runge-Kutta BUG integrator is bounded by*

$$\|\mathbf{Y}_k - \mathbf{Y}_0\|_F \leq g_{k-1}^* \frac{e^{kh\tilde{K}_0} - 1}{\tilde{K}_0}, \quad (14)$$

where $g_k^* = \max_{0 \leq l \leq k} g_l$ and $g_l = \sum_{i=1}^s \tilde{K}_i \|\mathbf{F}(t_{li}, \mathbf{Y}_0)\|_F$.

Proof. We start by showing by induction that

$$\|\mathbf{Y}_k - \mathbf{Y}_0\|_F \leq h \sum_{l=0}^{k-1} (1 + h\tilde{K}_0)^{k-1-l} g_l. \quad (15)$$

For $k = 0$, the statement is trivial. Then, for $k \geq 1$, Lemma 2 and the induction hypothesis lead to the desired result

$$\begin{aligned}\|\mathbf{Y}_{k+1} - \mathbf{Y}_0\|_F &\leq (1 + h\tilde{K}_0) \|\mathbf{Y}_k - \mathbf{Y}_0\|_F + hg_k \\ &\leq (1 + h\tilde{K}_0) \left(h \sum_{l=0}^{k-1} (1 + h\tilde{K}_0)^{k-1-l} g_l \right) + hg_k \\ &= h \sum_{l=0}^k (1 + h\tilde{K}_0)^{k-l} g_l.\end{aligned}$$

Finally, we deduce from equation (15) that

$$\begin{aligned}\|\mathbf{Y}_k - \mathbf{Y}_0\|_F &\leq hg_{k-1}^* \sum_{l=0}^{k-1} (1 + h\tilde{K}_0)^{k-1-l} \\ &= g_{k-1}^* \frac{(1 + h\tilde{K}_0)^k - 1}{\tilde{K}_0} \\ &\leq g_{k-1}^* \frac{e^{kh\tilde{K}_0} - 1}{\tilde{K}_0},\end{aligned}$$

which concludes the proof. □

According to Propositions 1 and 2, the exact solution $\mathbf{Y}(t)$ and the discrete solution of the Runge-Kutta BUG integrator are bounded on the finite time-interval $0 \leq t \leq T$. Let

$$\mathcal{V}_r := \{\mathbf{X} \in \mathcal{M}_r \mid \|\mathbf{X} - \mathbf{Y}_0\|_F \leq \max\{R_1, R_2\}\}, \quad (16)$$

where

$$R_1 = \int_0^T e^{L(T-t)} \|\mathbf{F}(t, \mathbf{Y}_0)\|_F dt,$$

$$R_2 = \max_{1 \leq i \leq s} \left\{ (1 + K_{i0}h_0) \left(\sum_{j=1}^s \tilde{K}_j \right) \frac{e^{T\tilde{K}_0} - 1}{\tilde{K}_0} + h_0 \sum_{j=1}^{i-1} K_{ij} \right\} \times \sup_{t \in [0, T]} \|\mathbf{F}(t, \mathbf{Y}_0)\|_F.$$

The subset $\mathcal{V}_r \subseteq \mathcal{M}_r$ is a neighbourhood of the exact solution $\mathbf{Y}(t)$ which contains the solution of the Runge-Kutta BUG integrator for all $t \in [0, T]$ and $h \leq h_0$. As a consequence, since $\mathbf{F}(t, \mathbf{X})$ is continuous in time and Lipschitz continuous in \mathbf{X} , \mathbf{F} is bounded on the compact set $[0, T] \times \mathcal{V}_r$, and there exists a constant $B \geq 0$ such that

$$\|\mathbf{F}(t, \mathbf{X})\|_F \leq B \quad (17)$$

for all $t \in [0, T]$ and $\mathbf{X} \in \mathcal{V}_r$.

Lemma 3. *Under Assumption 1, the exact flow is e^{Lt} -Lipschitz continuous:*

$$\|\Phi_{\mathbf{F}}^t(\mathbf{X}_1) - \Phi_{\mathbf{F}}^t(\mathbf{X}_2)\|_F \leq e^{Lt} \|\mathbf{X}_1 - \mathbf{X}_2\|_F \quad (18)$$

for all $t \in [0, T]$ and $\mathbf{X}_1, \mathbf{X}_2 \in \mathbb{R}^{n \times m}$.

Proof. From Assumption 1, we obtain the differential inequality

$$\begin{aligned} \frac{d}{dt} \|\Phi_{\mathbf{F}}^t(\mathbf{X}_1) - \Phi_{\mathbf{F}}^t(\mathbf{X}_2)\|_F^2 &= 2 \langle \Phi_{\mathbf{F}}^t(\mathbf{X}_1) - \Phi_{\mathbf{F}}^t(\mathbf{X}_2), \mathbf{F}(t, \Phi_{\mathbf{F}}^t(\mathbf{X}_1)) - \mathbf{F}(t, \Phi_{\mathbf{F}}^t(\mathbf{X}_2)) \rangle_F \\ &\leq 2L \|\Phi_{\mathbf{F}}^t(\mathbf{X}_1) - \Phi_{\mathbf{F}}^t(\mathbf{X}_2)\|_F^2 \end{aligned}$$

and, according to the Grönwall's inequality, the exact flow verifies

$$\|\Phi_{\mathbf{F}}^t(\mathbf{X}_1) - \Phi_{\mathbf{F}}^t(\mathbf{X}_2)\|_F^2 \leq e^{2Lt} \|\mathbf{X}_1 - \mathbf{X}_2\|_F^2,$$

which concludes the proof. \square

4.2 Error estimation

We now introduce several definitions and propositions that will be useful to prove the high-order convergence of the Runge-Kutta BUG integrator. In particular, Proposition 3 shows that the projection error resulting from the Galerkin projection of the Runge-Kutta BUG integrator is not larger than the one resulting from the tangent-space projection, which will allow us to adapt the convergence analysis of projected Runge-Kutta methods [28] to our Runge-Kutta BUG integrator. In addition, equation (27)

provides an estimate for the truncation error that will allow us to obtain error bounds with an improved order of convergence compared to [28].

Proposition 3. *The Galerkin projection of the Runge-Kutta BUG integrator is more accurate than the tangent-space projection for approximating $\mathbf{F}_{k,i}$:*

$$\left\| \mathbf{F}_{ki} - \widehat{\mathbf{U}}_{k+1} \widehat{\mathbf{U}}_{k+1}^T \mathbf{F}_{ki} \widehat{\mathbf{V}}_{k+1} \widehat{\mathbf{V}}_{k+1}^T \right\|_F \leq \left\| \mathbf{F}_{ki} - \mathcal{P}_{\mathbf{Y}_{ki}}(\mathbf{F}_{ki}) \right\|_F \quad (19)$$

for all $i \in \{1, \dots, s\}$ such that $b_i \neq 0$. Similarly, the projection error at each stage $i \in \{1, \dots, s-1\}$ verifies

$$\left\| \mathbf{F}_{kj} - \widehat{\mathbf{U}}_{k,i+1} \widehat{\mathbf{U}}_{k,i+1}^T \mathbf{F}_{kj} \widehat{\mathbf{V}}_{k,i+1} \widehat{\mathbf{V}}_{k,i+1}^T \right\|_F \leq \left\| \mathbf{F}_{kj} - \mathcal{P}_{\mathbf{Y}_{kj}}(\mathbf{F}_{kj}) \right\|_F \quad (20)$$

for all $j \in \{1, \dots, i\}$ such that $a_{i+1,j} \neq 0$.

Proof. We prove equation (19). The proof of equation (20) follows from the same arguments and is therefore omitted. Let the SVD of $\mathcal{P}_{\mathbf{Y}_{ki}}(\mathbf{F}_{ki})$ be $\Phi \Sigma \Psi^T$, where $\Phi \in \mathbb{R}^{n \times \bar{r}}$ and $\Psi \in \mathbb{R}^{m \times \bar{r}}$ are orthonormal matrices, $\Sigma \in \mathbb{R}^{\bar{r} \times \bar{r}}$ is a diagonal matrix with non-negative real numbers on the diagonal, and $\bar{r} \in \{r, \dots, \min\{n, m, 2r\}\}$. If $b_i \neq 0$, then the augmented bases $\widehat{\mathbf{U}}_{k+1}$ and $\widehat{\mathbf{V}}_{k+1}$ contain by construction the range of $[\mathbf{U}_{ki} \ \mathbf{F}_{ki} \ \mathbf{V}_{ki}]$ and $[\mathbf{V}_{ki} \ \mathbf{F}_{ki}^T \ \mathbf{U}_{ki}]$, respectively, and it follows that the left and right singular vectors of $\mathcal{P}_{\mathbf{Y}_{ki}}(\mathbf{F}_{ki})$ are included in the span of the augmented bases:

$$\Phi \subseteq \text{span}(\widehat{\mathbf{U}}_{k+1}) \quad \text{and} \quad \Psi \subseteq \text{span}(\widehat{\mathbf{V}}_{k+1}),$$

where $\widehat{\mathbf{U}}_{k+1} \in \mathbb{R}^{n \times \hat{r}}$, $\widehat{\mathbf{V}}_{k+1} \in \mathbb{R}^{m \times \hat{r}}$, and $\hat{r} \in \{\bar{r}, \dots, \min\{n, m, 2rs\}\}$. Consequently, the Galerkin projection onto the augmented bases verifies

$$\begin{aligned} \left\| \mathbf{F}_{ki} - \mathcal{P}_{\mathbf{Y}_{ki}}(\mathbf{F}_{ki}) \right\|_F &= \left\| \mathbf{F}_{ki} - \Phi \Sigma \Psi^T \right\|_F \\ &\geq \min_{\Sigma \in \mathbb{R}^{\bar{r} \times \bar{r}}} \left\| \mathbf{F}_{ki} - \Phi \Sigma \Psi^T \right\|_F \\ &\geq \min_{\widehat{\Sigma} \in \mathbb{R}^{\hat{r} \times \hat{r}}} \left\| \mathbf{F}_{ki} - \widehat{\mathbf{U}}_{k+1} \widehat{\Sigma} \widehat{\mathbf{V}}_{k+1}^T \right\|_F \\ &= \left\| \mathbf{F}_{ki} - \widehat{\mathbf{U}}_{k+1} \widehat{\mathbf{U}}_{k+1}^T \mathbf{F}_{ki} \widehat{\mathbf{V}}_{k+1} \widehat{\mathbf{V}}_{k+1}^T \right\|_F, \end{aligned}$$

which concludes the proof. \square

Since \mathbf{F} is bounded on $[0, T] \times \mathcal{V}_r$, the orthogonal projection of \mathbf{F} onto the tangent space is also bounded on $[0, T] \times \mathcal{V}_r$, and there exists $\varepsilon_r \geq 0$ such that the tangent-space projection error is bounded on $[0, T] \times \mathcal{V}_r$. Let

$$\varepsilon_r := \sup_{t \in [0, T]} \sup_{\mathbf{X} \in \mathcal{V}_r} \left\| \mathbf{F}(t, \mathbf{X}) - \mathcal{P}_{\mathbf{X}}(\mathbf{F}(t, \mathbf{X})) \right\|_F. \quad (21)$$

It follows from Proposition 3 that the projection error of the Runge-Kutta BUG integrator is bounded by ε_r :

$$\left\| \mathbf{F}_{ki} - \widehat{\mathbf{U}}_{k+1} \widehat{\mathbf{U}}_{k+1}^T \mathbf{F}_{ki} \widehat{\mathbf{V}}_{k+1} \widehat{\mathbf{V}}_{k+1}^T \right\|_F \leq \varepsilon_r$$

for all $i \in \{1, \dots, s\}$ such that $b_i \neq 0$, and

$$\left\| \mathbf{F}_{kj} - \widehat{\mathbf{U}}_{k,i+1} \widehat{\mathbf{U}}_{k,i+1}^T \mathbf{F}_{kj} \widehat{\mathbf{V}}_{k,i+1} \widehat{\mathbf{V}}_{k,i+1}^T \right\|_F \leq \varepsilon_r$$

for all $j \in \{1, \dots, i\}$ such that $a_{i+1,j} \neq 0$. In addition, note that the tangent-space projection error and therefore ε_r vanish when $r = \min\{n, m\}$.

Proposition 4. *Suppose that Assumption 1 holds. Then, for $[t_k, t_{k+1}] \subseteq [0, T]$ and $h \leq h_0$, the error resulting from the truncation step of the Runge-Kutta BUG integrator is proportional to h : the ratio*

$$\frac{1}{h} \left\| \widehat{\mathbf{Y}}_{k+1} - \left[\widehat{\mathbf{Y}}_{k+1} \right]_r \right\|_F \quad (22)$$

is bounded independently of h . Similarly, at each stage $i \in \{1, \dots, s-1\}$, the truncation error is proportional to h : the ratio

$$\frac{1}{h} \left\| \widehat{\mathbf{Y}}_{k,i+1} - \left[\widehat{\mathbf{Y}}_{k,i+1} \right]_r \right\|_F \quad (23)$$

is bounded independently of h .

Proof. We prove equation (22). The proof of equation (23) follows from the same arguments and is therefore omitted. Let $\sigma_j(\mathbf{X})$ denote the j -th largest singular value of the matrix $\mathbf{X} \in \mathbb{R}^{n \times m}$. The squared truncation error is given according to the Eckart-Young theorem [34] by

$$\left\| \widehat{\mathbf{Y}}_{k+1} - \left[\widehat{\mathbf{Y}}_{k+1} \right]_r \right\|_F^2 = \sum_{j=r+1}^{\min\{n,m,2rs\}} \sigma_j^2(\widehat{\mathbf{Y}}_{k+1}), \quad (24)$$

since the rank of $\widehat{\mathbf{Y}}_{k+1}$ is at most $2rs$ (see Remark 1) and, consequently, $\sigma_j^2(\widehat{\mathbf{Y}}_{k+1}) = 0$ for $j > 2rs$. Then, as

$$\widehat{\mathbf{Y}}_{k+1} = \mathbf{Y}_k + h \left(b_1 \widetilde{\mathbf{F}}_{k1} + \dots + b_s \widetilde{\mathbf{F}}_{ks} \right) \quad \text{with} \quad \widetilde{\mathbf{F}}_{ki} = \widehat{\mathbf{U}}_{k+1} \widehat{\mathbf{U}}_{k+1}^T \mathbf{F}_{ki} \widehat{\mathbf{V}}_{k+1} \widehat{\mathbf{V}}_{k+1}^T,$$

the singular values of $\widehat{\mathbf{Y}}_{k+1}$ are bounded according to Theorem 3.3.16 in [35] by

$$\sigma_{i+j-1}(\widehat{\mathbf{Y}}_{k+1}) \leq \sigma_i(\mathbf{Y}_k) + h \sigma_j(b_1 \widetilde{\mathbf{F}}_{k1} + \dots + b_s \widetilde{\mathbf{F}}_{ks})$$

for all $i \in \{1, \dots, \min\{n, m, 2r\}\}$ and $j \in \{1, \dots, \min\{n, m, 2rs\}\}$ such that $i+j-1 \leq \min\{n, m, 2rs\}$. In particular, for $i = r+1$ and $j \geq 1$, it follows that

$$\sigma_{r+j}(\widehat{\mathbf{Y}}_{k+1}) \leq h\sigma_j(b_1\widetilde{\mathbf{F}}_{k1} + \dots + b_s\widetilde{\mathbf{F}}_{ks}), \quad (25)$$

since the rank of \mathbf{Y}_k is at most r . Moreover, we deduce from equation (17) that

$$\begin{aligned} \sum_{j=1}^{\min\{n, m, 2rs\}} \sigma_j^2(b_1\widetilde{\mathbf{F}}_{k1} + \dots + b_s\widetilde{\mathbf{F}}_{ks}) &= \left\| b_1\widetilde{\mathbf{F}}_{k1} + \dots + b_s\widetilde{\mathbf{F}}_{ks} \right\|_F^2 \\ &\leq \left(|b_1| \left\| \widetilde{\mathbf{F}}_{k1} \right\|_F + \dots + |b_s| \left\| \widetilde{\mathbf{F}}_{ks} \right\|_F \right)^2 \\ &\leq \left(|b_1| \left\| \mathbf{F}_{k1} \right\|_F + \dots + |b_s| \left\| \mathbf{F}_{ks} \right\|_F \right)^2 \\ &\leq \left(|b_1|B + \dots + |b_s|B \right)^2 \\ &= C_B^2 B^2 \end{aligned}$$

and, consequently,

$$\sigma_j^2(b_1\widetilde{\mathbf{F}}_{k1} + \dots + b_s\widetilde{\mathbf{F}}_{ks}) \leq C_B^2 B^2, \quad j \geq 1, \quad (26)$$

where $C_B = \sum_{i=1}^s |b_i|$. Finally, combining equations (24), (25), and (26) yields

$$\begin{aligned} \left\| \widehat{\mathbf{Y}}_{k+1} - \left[\widehat{\mathbf{Y}}_{k+1} \right]_r \right\|_F^2 &= \sum_{j=1}^{\min\{n, m, 2rs\} - r} \sigma_{r+j}^2(\widehat{\mathbf{Y}}_{k+1}) \\ &\leq \sum_{j=1}^{\min\{n, m, 2rs\} - r} h^2 \sigma_j^2(b_1\widetilde{\mathbf{F}}_{k1} + \dots + b_s\widetilde{\mathbf{F}}_{ks}) \\ &\leq \sum_{j=1}^{\min\{n, m, 2rs\} - r} h^2 C_B^2 B^2 \\ &= h^2 (\min\{n, m, 2rs\} - r) C_B^2 B^2. \end{aligned}$$

The desired result follows directly from the fact that the term $(\min\{n, m, 2rs\} - r)C_B^2 B^2$ is finite and does not depend on h . \square

According to Proposition 4, there exists $\gamma_r \geq 0$ such that the ratios (22) and (23) are bounded. Let

$$\gamma_r := \max \left\{ \sup_{t_{k,i+1} \in [0, T]} \sup_{\mathbf{x}_k \in \mathcal{V}_r} \frac{1}{h} \left\| \widehat{\mathbf{X}}_{k,i+1} - \left[\widehat{\mathbf{X}}_{k,i+1} \right]_r \right\|_F, \right. \\ \left. \sup_{t_{k+1} \in [0, T]} \sup_{\mathbf{x}_k \in \mathcal{V}_r} \frac{1}{h} \left\| \widehat{\mathbf{X}}_{k+1} - \left[\widehat{\mathbf{X}}_{k+1} \right]_r \right\|_F \right\}, \quad (27)$$

where $\widehat{\mathbf{X}}_{k+1}$ and $\widehat{\mathbf{X}}_{k,i+1}$ denote the augmented solutions computed by the Runge-Kutta BUG integrator using the initial value \mathbf{X}_k at time t_k . It follows that the truncation error is bounded by

$$\begin{aligned} \left\| \widehat{\mathbf{Y}}_{k,i+1} - \left[\widehat{\mathbf{Y}}_{k,i+1} \right]_r \right\|_F &\leq h\gamma_r, \quad i = 1, \dots, s-1, \\ \left\| \widehat{\mathbf{Y}}_{k+1} - \left[\widehat{\mathbf{Y}}_{k+1} \right]_r \right\|_F &\leq h\gamma_r. \end{aligned}$$

In addition, note that the truncation error and therefore γ_r vanish when $r = \min\{n, m\}$.

Remark 3. In general, γ_r is not related to ε_r , but in some cases the truncation error can be bounded by using ε_r . For instance, according to the proof of Proposition 4, if

$$\sigma_1(\widetilde{\mathbf{F}}_{ki}) \leq \varepsilon_r, \quad \forall t_{k,i} \in [0, T], \quad (28)$$

then it holds

$$\begin{aligned} \sigma_1(a_{i+1,1}\widetilde{\mathbf{F}}_{k1} + \dots + a_{i,i+1}\widetilde{\mathbf{F}}_{ki}) &\leq C_A\varepsilon_r, \quad \forall t_{ki} \in [0, T], \\ \sigma_1(b_1\widetilde{\mathbf{F}}_{k1} + \dots + b_s\widetilde{\mathbf{F}}_{ks}) &\leq C_B\varepsilon_r, \quad \forall t_{k+1} \in [0, T], \end{aligned}$$

and one can take $\gamma_r = \max\{C_A, C_B\}\varepsilon_r$ with $C_A = \sum_{i,j=1}^s |a_{ij}|$ and $C_B = \sum_{i=1}^s |b_i|$. In particular, condition (28) for a specific time t_{ki} is satisfied if the left and right singular vectors associated with the largest singular value of \mathbf{F}_{ki} are not included in the left and right singular vectors of $\mathcal{P}_{\mathbf{Y}_{ki}}(\mathbf{F}_{ki})$, which is however unlikely, especially if $\mathcal{P}_{\mathbf{Y}_{ki}}(\mathbf{F}_{ki})$ is a good approximation of \mathbf{F}_{ki} .

Proposition 5. Let the Runge-Kutta method (10) be a numerical scheme of order p , and suppose that Assumption 2 holds. Then, for $h \leq h_0$, the local error of the Runge-Kutta method verifies

$$\left\| \mathbf{A}_{k+1} - \Phi_{\mathbf{F}}^h(\mathbf{A}_k) \right\|_F \leq C_L h^{p+1}, \quad (29)$$

where the constant $C_L > 0$ is independent of h .

Proof. see Theorem 3.1 of Chapter 2 in [33]. □

4.3 Local and global error bounds

We establish the local and global error bounds in Theorems 1 and 2, respectively. These error bounds show that the proposed Runge-Kutta BUG integrator retains the order of convergence of the associated Runge-Kutta method until the error reaches a plateau corresponding to the low-rank truncation error and which vanishes as the rank becomes full. Compared to [28], we obtain local and global error bounds with an improved order of convergence in h thanks to the introduction of the additional error term γ_r , but similar error bounds can be obtained for projected Runge-Kutta methods by introducing such error term and adapting the convergence analysis accordingly.

Lemma 4. *Suppose that Assumption 1 holds, and consider the time subinterval $[t_k, t_{k+1}] \subseteq [0, T]$. Moreover, let \mathbf{Z}_{ki} denote the discrete solution computed using the (unprojected) Runge-Kutta method (10) with the initial value $\mathbf{Z}_k = \mathbf{Y}_k \in \mathcal{M}_r$. Then, for $h \leq h_0$, it holds*

$$\|\mathbf{Y}_{ki} - \mathbf{Z}_{ki}\|_F \leq C_i h(\varepsilon_r + \gamma_r), \quad i = 1, \dots, s, \quad (30)$$

where the constant $C_i \geq 0$ is independent of h and r .

Proof. We proceed by induction. For $i = 1$, the statement is trivial with $C_1 = 0$ since $\mathbf{Z}_{k1} = \mathbf{Z}_k = \mathbf{Y}_k = \mathbf{Y}_{k1}$. Then, for $i \in \{2, \dots, s\}$, the local error can be split into

$$\|\mathbf{Y}_{ki} - \mathbf{Z}_{ki}\|_F \leq \left\| \mathbf{Y}_{ki} - \widehat{\mathbf{Y}}_{ki} \right\|_F + \left\| \widehat{\mathbf{Y}}_{ki} - \mathbf{Z}_{ki} \right\|_F. \quad (31)$$

The first term in the RHS is bounded by

$$\left\| \widehat{\mathbf{Y}}_{ki} - \mathbf{Y}_{ki} \right\|_F \leq h\gamma_r. \quad (32)$$

Regarding the second term, we deduce from the induction hypothesis that

$$\begin{aligned} \left\| \widehat{\mathbf{Y}}_{ki} - \mathbf{Z}_{ki} \right\|_F &\leq h \sum_{j=1}^{i-1} |a_{ij}| \left\| \widehat{\mathbf{U}}_{ki} \widehat{\mathbf{U}}_{ki}^T \mathbf{F}(t_{kj}, \mathbf{Y}_{kj}) \widehat{\mathbf{V}}_{ki} \widehat{\mathbf{V}}_{ki}^T - \mathbf{F}(t_{kj}, \mathbf{Z}_{kj}) \right\|_F \\ &= h \sum_{j \in \mathcal{I}_A} |a_{ij}| \left\| \widehat{\mathbf{U}}_{ki} \widehat{\mathbf{U}}_{ki}^T \mathbf{F}(t_{kj}, \mathbf{Y}_{kj}) \widehat{\mathbf{V}}_{ki} \widehat{\mathbf{V}}_{ki}^T - \mathbf{F}(t_{kj}, \mathbf{Z}_{kj}) \right\|_F \\ &\leq h \sum_{j \in \mathcal{I}_A} |a_{ij}| \left(\left\| \widehat{\mathbf{U}}_{ki} \widehat{\mathbf{U}}_{ki}^T \mathbf{F}(t_{kj}, \mathbf{Y}_{kj}) \widehat{\mathbf{V}}_{ki} \widehat{\mathbf{V}}_{ki}^T - \mathbf{F}(t_{kj}, \mathbf{Y}_{kj}) \right\|_F \right. \\ &\quad \left. + \left\| \mathbf{F}(t_{kj}, \mathbf{Y}_{kj}) - \mathbf{F}(t_{kj}, \mathbf{Z}_{kj}) \right\|_F \right) \\ &\leq h \sum_{j \in \mathcal{I}_A} |a_{ij}| (\varepsilon_r + L \|\mathbf{Y}_{kj} - \mathbf{Z}_{kj}\|_F) \\ &\leq \left(\sum_{j \in \mathcal{I}_A} |a_{ij}| (1 + LC_j h) \right) h \varepsilon_r + \left(\sum_{j \in \mathcal{I}_A} |a_{ij}| LC_j \right) h^2 \gamma_r, \end{aligned} \quad (33)$$

where $\mathcal{I}_A = \{j \in \{1, \dots, i-1\} \mid a_{ij} \neq 0\}$. Finally, combining equations (31), (32), and (33) yields the desired result:

$$\begin{aligned} \|\mathbf{Y}_{ki} - \mathbf{Z}_{ki}\|_F &\leq \left(\sum_{j \in \mathcal{I}_A} |a_{ij}| (1 + LC_j h) \right) h \varepsilon_r + \left(1 + \sum_{j \in \mathcal{I}_A} |a_{ij}| LC_j h \right) h \gamma_r \\ &\leq C_i h (\varepsilon_r + \gamma_r), \end{aligned}$$

where $C_1 = 0$ and $C_i = \max \left\{ \sum_{j=1}^{i-1} |a_{ij}| (1 + LC_j h_0), 1 + \sum_{j=1}^{i-1} |a_{ij}| LC_j h_0 \right\}$ for $i = 2, \dots, s$. \square

Theorem 1. *Suppose that Assumptions 1 and 2 hold, and consider the time subinterval $[t_k, t_{k+1}] \subseteq [0, T]$. Then, for $h \leq h_0$, the local error of the Runge-Kutta BUG integrator verifies*

$$\|\mathbf{Y}_{k+1} - \Phi_{\mathbf{F}}^h(\mathbf{Y}_k)\|_F \leq Ch(\varepsilon_r + \gamma_r + h^p), \quad (34)$$

where the constant $C > 0$ is independent of h and r .

Proof. Let \mathbf{Z}_{k+1} denote the discrete solution computed using the Runge-Kutta method (10) with the initial value $\mathbf{Z}_k = \mathbf{Y}_k \in \mathcal{M}_r$. The local error can be split into

$$\|\mathbf{Y}_{k+1} - \Phi_{\mathbf{F}}^h(\mathbf{Y}_k)\|_F \leq \|\mathbf{Y}_{k+1} - \widehat{\mathbf{Y}}_{k+1}\|_F + \|\widehat{\mathbf{Y}}_{k+1} - \mathbf{Z}_{k+1}\|_F + \|\mathbf{Z}_{k+1} - \Phi_{\mathbf{F}}^h(\mathbf{Y}_k)\|_F. \quad (35)$$

The first term in the RHS is bounded by

$$\|\widehat{\mathbf{Y}}_{k+1} - \mathbf{Y}_{k+1}\|_F \leq h\gamma_r. \quad (36)$$

Regarding the second term, we deduce from Lemma 4 that

$$\begin{aligned} \|\widehat{\mathbf{Y}}_{k+1} - \mathbf{Z}_{k+1}\|_F &\leq h \sum_{i=1}^s |b_i| \left\| \widehat{\mathbf{U}}_{k+1} \widehat{\mathbf{U}}_{k+1}^T \mathbf{F}(t_{ki}, \mathbf{Y}_{ki}) \widehat{\mathbf{V}}_{k+1} \widehat{\mathbf{V}}_{k+1}^T - \mathbf{F}(t_{ki}, \mathbf{Z}_{ki}) \right\|_F \\ &= h \sum_{i \in \mathcal{I}_B} |b_i| \left\| \widehat{\mathbf{U}}_{k+1} \widehat{\mathbf{U}}_{k+1}^T \mathbf{F}(t_{ki}, \mathbf{Y}_{ki}) \widehat{\mathbf{V}}_{k+1} \widehat{\mathbf{V}}_{k+1}^T - \mathbf{F}(t_{ki}, \mathbf{Z}_{ki}) \right\|_F \\ &\leq h \sum_{i \in \mathcal{I}_B} |b_i| \left(\left\| \widehat{\mathbf{U}}_{k+1} \widehat{\mathbf{U}}_{k+1}^T \mathbf{F}(t_{ki}, \mathbf{Y}_{ki}) \widehat{\mathbf{V}}_{k+1} \widehat{\mathbf{V}}_{k+1}^T - \mathbf{F}(t_{ki}, \mathbf{Y}_{ki}) \right\|_F \right. \\ &\quad \left. + \|\mathbf{F}(t_{ki}, \mathbf{Y}_{ki}) - \mathbf{F}(t_{ki}, \mathbf{Z}_{ki})\|_F \right) \\ &\leq h \sum_{i \in \mathcal{I}_B} |b_i| (\varepsilon_r + L \|\mathbf{Y}_{ki} - \mathbf{Z}_{ki}\|_F) \\ &\leq \left(\sum_{i \in \mathcal{I}_B} |b_i| (1 + LC_i h) \right) h \varepsilon_r + \left(\sum_{i \in \mathcal{I}_B} |b_i| LC_i \right) h^2 \gamma_r \end{aligned} \quad (37)$$

where $\mathcal{I}_B = \{i \in \{1, \dots, s\} \mid b_i \neq 0\}$. The last term is bounded according to Proposition 5 by

$$\|\mathbf{Z}_{k+1} - \Phi_{\mathbf{F}}^h(\mathbf{Y}_k)\|_F = \|\mathbf{Z}_{k+1} - \Phi_{\mathbf{F}}^h(\mathbf{Z}_k)\|_F \leq C_L h^{p+1}. \quad (38)$$

Finally, combining equations (35), (36), (37), and (38) yields the desired result:

$$\begin{aligned} \|\mathbf{Y}_{k+1} - \Phi_{\mathbf{F}}^h(\mathbf{Y}_k)\|_F &\leq \left(\sum_{i \in \mathcal{I}_B} |b_i| (1 + LC_i h) \right) h \varepsilon_r + \left(1 + \sum_{i \in \mathcal{I}_B} |b_i| LC_i h \right) h \gamma_r + C_L h^{p+1} \\ &\leq Ch(\varepsilon_r + \gamma_r + h^p), \end{aligned}$$

where $C = \max \left\{ \sum_{i=1}^s |b_i|(1 + LC_i h_0), 1 + \sum_{i=1}^s |b_i| LC_i h_0, C_L \right\}$. \square

Theorem 2. *Let the initial error be $\delta_r = \|\mathbf{Y}_0 - \mathbf{A}_0\|_F$ with δ_r vanishing when $r = \min\{n, m\}$. Moreover, suppose that Assumptions 1 and 2 hold. Then, for $h \leq h_0$, the global error of the Runge-Kutta BUG integrator verifies*

$$\|\mathbf{Y}_N - \mathbf{A}(t_N)\|_F \leq C' (\delta_r + \varepsilon_r + \gamma_r + h^p), \quad (39)$$

on the finite time-interval $0 \leq t_N \leq T$. The constant $C' > 0$ depends on $T, L, C_L, h_0, C_A = \sum_{i,j=1}^s |a_{ij}|$, and $C_B = \sum_{i=1}^s |b_i|$ but not on h nor r .

Proof. The bound results from the local error of Theorem 1 and the standard argument of Lady Windermere's fan with error propagation along the exact flow. More specifically, the global error can be expanded as the telescoping sum

$$\mathbf{Y}_N - \Phi_{\mathbf{F}}^{Nh}(\mathbf{A}_0) = \left(\sum_{k=1}^N \Phi_{\mathbf{F}}^{(N-k)h}(\mathbf{Y}_k) - \Phi_{\mathbf{F}}^{(N-k+1)h}(\mathbf{Y}_{k-1}) \right) + \Phi_{\mathbf{F}}^{Nh}(\mathbf{Y}_0) - \Phi_{\mathbf{F}}^{Nh}(\mathbf{A}_0).$$

Then, the different terms can be bounded according to Lemma 3 and Theorem 1 by

$$\begin{aligned} \|\Phi_{\mathbf{F}}^{Nh}(\mathbf{Y}_0) - \Phi_{\mathbf{F}}^{Nh}(\mathbf{A}_0)\|_F &\leq e^{LNh} \|\mathbf{Y}_0 - \mathbf{A}_0\|_F = e^{LNh} \delta_r, \\ \left\| \Phi_{\mathbf{F}}^{(N-k)h}(\mathbf{Y}_k) - \Phi_{\mathbf{F}}^{(N-k)h}(\Phi_{\mathbf{F}}^h(\mathbf{Y}_{k-1})) \right\|_F &\leq e^{L(N-k)h} \|\mathbf{Y}_k - \Phi_{\mathbf{F}}^h(\mathbf{Y}_{k-1})\|_F \\ &\leq e^{L(N-k)h} Ch(\varepsilon_r + \gamma_r + h^p), \end{aligned}$$

which leads to the upper bound:

$$\|\mathbf{Y}_N - \Phi_{\mathbf{F}}^{Nh}(\mathbf{A}_0)\|_F \leq e^{LNh} \delta_r + C(\varepsilon_r + \gamma_r + h^p) \sum_{k=1}^N e^{L(N-k)h} h.$$

Finally, bounding the Riemann sum as

$$\sum_{k=1}^N h e^{L(N-k)h} \leq \int_0^{Nh} e^{L(Nh-t)} dt = \frac{e^{LNh} - 1}{L}$$

and using $Nh \leq T$ lead to

$$\begin{aligned} \|\mathbf{Y}_N - \Phi_{\mathbf{F}}^{Nh}(\mathbf{A}_0)\|_F &\leq e^{LT} \delta_r + C \frac{e^{LT} - 1}{L} (\varepsilon_r + \gamma_r + h^p) \\ &\leq \max \left\{ e^{LT}, C \frac{e^{LT} - 1}{L} \right\} (\delta_r + \varepsilon_r + \gamma_r + h^p), \end{aligned}$$

which concludes the proof. \square

Remark 4. *If $\max\{\delta_r, \varepsilon_r, \gamma_r\} \ll h^p$, then the Runge-Kutta BUG integrator has the same order of convergence as the associated Runge-Kutta method. Otherwise, the global error is dominated by the low-rank truncation error (namely the initial, projection, and truncation errors) and vanishes as the rank becomes full.*

5 Numerical experiments

According to Theorem 2, the rate of convergence of the proposed Runge-Kutta BUG integrator scales with h^p until the error reaches a plateau which decreases as the rank increases. This theoretical result is validated experimentally on three numerical test cases taken from [28, 36]. To this end, we investigate the convergence of several Runge-Kutta BUG integrators based on the following high-order explicit Runge-Kutta methods:

- midpoint method (RK2m),
- Heun’s method (RK2h),
- Heun’s third-order method (RK3h),
- third-order SSP RK method (RK3s),
- classic fourth-order Runge-Kutta method (RK4),

where the associated Butcher tableaux are given in Appendix A. The accuracy of the resulting integrators is measured with respect to a reference solution \mathbf{A}_k computed using the fifth-order Runge-Kutta-Fehlberg method:

$$\text{Error} = \max_{k=0, \dots, N} \|\mathbf{Y}_k - \mathbf{A}_k\|_F.$$

Moreover, we compare these Runge-Kutta BUG integrators with the following state-of-the-art dynamical low-rank integrators:

- the first variant of the second-order BUG integrator (Midpoint BUG) of [30],
- the second-order projected Runge-Kutta method (PRK2h) [28],
- the third-order projected Runge-Kutta method (PRK3h) [28].

Notably, we consider the first variant of the midpoint BUG integrator [30] because it is more accurate than the second variant. In addition, this integrator is different from our Runge-Kutta BUG integrator based on the midpoint method since the intermediate solution is not truncated (the rank of $\widehat{\mathbf{Y}}_{k+1}$ is at most $4r$ instead of $2r$ in our Runge-Kutta BUG integrator). As a result, this integrator is computationally more expensive than our Runge-Kutta BUG integrator, but it is potentially more accurate. Note that the accuracy of these two integrators is almost the same in the following experiments.

5.1 Allen-Cahn equation

We first consider the Allen-Cahn equation:

$$\begin{cases} \dot{\mathbf{A}}(t) = \theta(\mathbf{L}\mathbf{A}(t) + \mathbf{A}(t)\mathbf{L}) + \mathbf{A}(t) - \mathbf{A}(t) \odot \mathbf{A}(t) \odot \mathbf{A}(t) \\ \mathbf{A}(0) = \mathbf{A}_0, \end{cases}$$

where $\mathbf{A}(t) \in \mathbb{R}^{n \times n}$, $\mathbf{L} = \frac{n^2}{4\pi^2} \text{diag}(1, -2, 1) \in \mathbb{R}^{n \times n}$, $t \in [0, 10]$, $\theta = 10^{-2}$, and \odot stands for the Hadamard product. The domain $[0, 2\pi]^2$ is discretized using $n = 128$ equidistant points in each direction, and the initial solution is given by

$$(\mathbf{A}_0)_{i,j} = \frac{\left[e^{-\tan^2(x_i)} + e^{-\tan^2(y_j)} \right] \sin(x_i) \sin(y_j)}{1 + e^{|\csc(-x_i/2)|} + e^{|\csc(-y_j/2)|}}.$$

In Figure 1, we present the error of the Runge-Kutta BUG integrator as a function of the time-step size h and rank r . The reader can see that the Runge-Kutta BUG integrator achieves second-, third-, and fourth-order convergences until the error reaches a plateau corresponding to the low-rank truncation error. This plateau decreases as the rank increases up to a certain limit, around 10^{-9} , resulting from the accumulation of roundoff error. In this example, the errors of the midpoint BUG integrator and projected Runge-Kutta methods are almost identical to those of our corresponding Runge-Kutta BUG integrators.

5.2 Lyapunov equation

Then, we consider the Lyapunov equation:

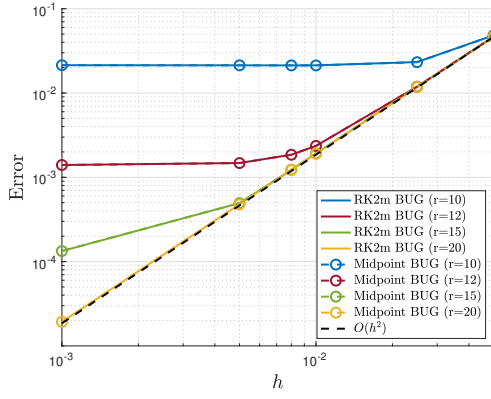
$$\begin{cases} \dot{\mathbf{A}}(t) = \mathbf{L}\mathbf{A}(t) + \mathbf{A}(t)\mathbf{L} + \theta \frac{\mathbf{C}}{\|\mathbf{C}\|_F} \\ \mathbf{A}(0) = \mathbf{A}_0, \end{cases}$$

where $\mathbf{A}(t) \in \mathbb{R}^{n \times n}$, $\mathbf{L} = \frac{n^2}{4\pi^2} \text{diag}(1, -2, 1) \in \mathbb{R}^{n \times n}$, $\mathbf{C} \in \mathbb{R}^{n \times n}$, $t \in [0, 1]$, and $\theta \geq 0$. The domain $[-\pi, \pi]^2$ is discretized using $n = 128$ equidistant points in each direction, and the initial solution and forcing term are given by

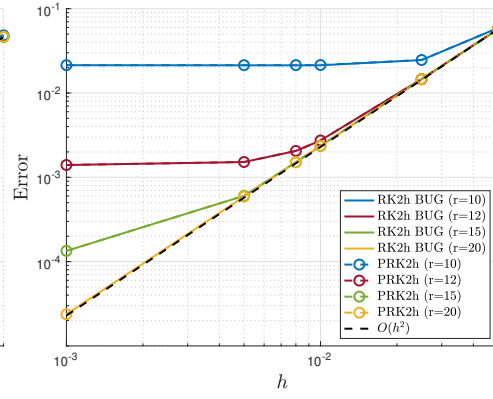
$$(\mathbf{A}_0)_{ij} = \sin(x_i) \sin(y_j) \quad \text{and} \quad (\mathbf{C})_{ij} = \sum_{l=1}^{11} 10^{-(l-1)} e^{-l(x_i^2 + y_j^2)}.$$

We start with the case $\theta = 10^{-5}$. In Figure 2, we fix the rank to $r = 5$ and we report the error of the Runge-Kutta BUG integrator as a function of the time-step size h . The reader can see that the proposed dynamical low-rank integrator achieves second- and third-order convergences until the error reaches a limit, around 10^{-10} , resulting from roundoff errors. Regarding the fourth-order convergence, this one is not visible since the error is already of the order of 10^{-11} for $h = 5 \times 10^{-4}$. Moreover, the errors of the midpoint BUG integrator and projected Runge-Kutta methods are almost the same as those of the corresponding Runge-Kutta BUG integrators for second-order methods. However, for the Heun's third-order method, the Runge-Kutta BUG integrator is significantly more accurate than the projected Runge-Kutta method.

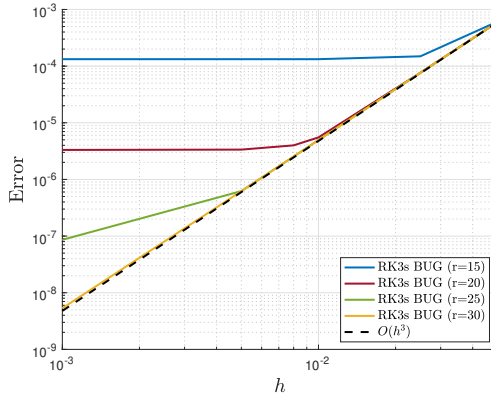
We now consider the case $\theta = 1$, where a higher rank is necessary to obtain a small rank truncation error due to the forcing term. In Figure 3, we see that the Runge-Kutta BUG integrator achieves second-order convergence. The third- and fourth-order



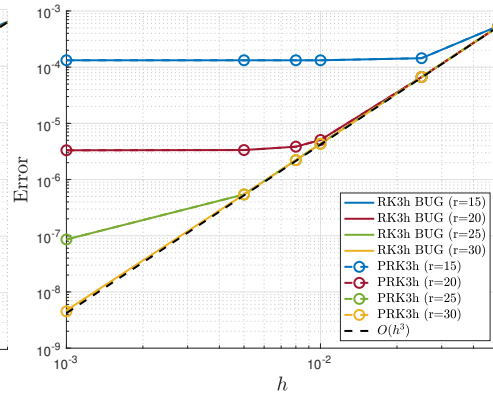
(a) Midpoint method



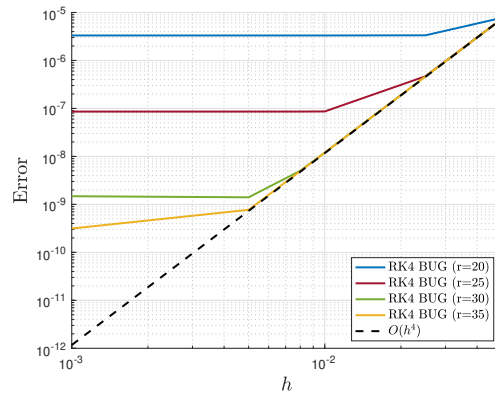
(b) Heun's method



(c) Third-order SSP Runge-Kutta method



(d) Heun's third-order method



(e) Classic fourth-order Runge-Kutta method

Fig. 1: Convergence error of the Runge-Kutta BUG integrator for the Allen-Cahn equation

convergences are not visible because the error, around 10^{-10} , is of the order of the cumulative roundoff error. Moreover, for second-order methods, the error reaches a plateau corresponding to the low-rank truncation error and which decreases as the rank increases. Furthermore, the Runge-Kutta BUG integrator is several orders of magnitude more accurate than the projected Runge-Kutta method, which can be explained by the fact that the Galerkin projection is more accurate than the tangent-space projection for approximating the discrete solution.

5.3 Discrete nonlinear Schrödinger equation

Lastly, we consider the discrete nonlinear Schrödinger equation [37]:

$$\begin{cases} i\dot{\mathbf{A}}(t) = -\frac{1}{2}(\mathbf{D}\mathbf{A}(t) + \mathbf{A}(t)\mathbf{D}) - \theta|\mathbf{A}(t)|^2 \odot \mathbf{A}(t) \\ \mathbf{A}(0) = \mathbf{A}_0, \end{cases}$$

where $\mathbf{A}(t) \in \mathbb{R}^{n \times n}$, $\mathbf{D} = \text{diag}(1, 0, 1) \in \mathbb{R}^{n \times n}$, $t \in [0, 5]$, and $\theta \geq 0$. Moreover, we set $n = 128$, and the initial solution is given by

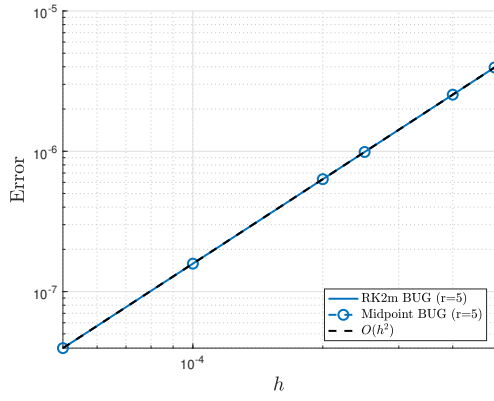
$$(\mathbf{A}_0)_{jl} = \exp\left(-\frac{(j-60)^2}{100} - \frac{(l-50)^2}{100}\right) + \exp\left(-\frac{(j-50)^2}{100} - \frac{(l-40)^2}{100}\right).$$

We start with the case $\theta = 0.1$. In Figure 4, we present the error of the Runge-Kutta BUG integrator as a function of the time-step size h and rank r . The reader can see that the Runge-Kutta BUG integrator achieves the expected orders of convergence. Then, the error reaches the plateau resulting from the low-rank truncation error and which decreases as the rank increases. Moreover, the errors of the midpoint BUG integrator and projected Runge-Kutta methods are almost the same as those of the corresponding Runge-Kutta BUG integrators for second-order methods. However, for the Heun's third-order method, the Runge-Kutta BUG integrator is significantly more accurate than the projected Runge-Kutta method.

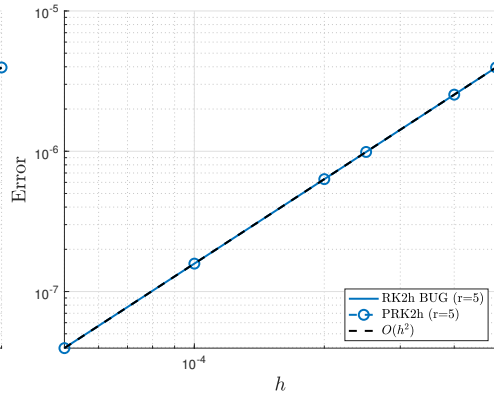
We now consider the case $\theta = 0.3$, where a higher rank is necessary to obtain small rank truncation errors due to the cubic term. In Figure 5, we see that the error behaves in the same way as before. Note that, for third-order methods, the Runge-Kutta BUG integrator achieves third-order convergence for $h \leq 10^{-1}$.

6 Conclusion

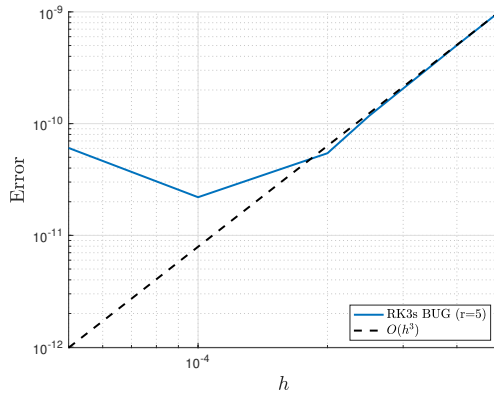
In this work, we have proposed high-order BUG integrators based on explicit Runge-Kutta methods. By construction, the resulting dynamical low-rank integrators are robust to the presence of small singular values and do not involve backward time-integration steps. Then, we have analyzed the convergence of the proposed Runge-Kutta BUG integrator. The error bound shows that the Runge-Kutta BUG integrator retains the order of convergence of the associated Runge-Kutta method until the error reaches a plateau corresponding to the low-rank truncation error and which vanishes as the rank becomes full. This error bound has been validated experimentally on three



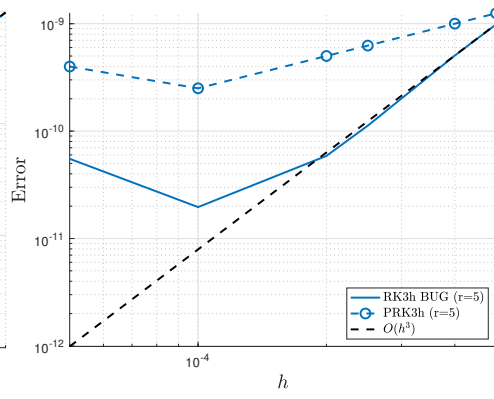
(a) Midpoint method



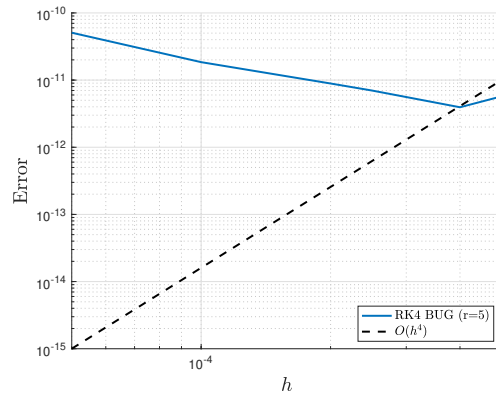
(b) Heun's method



(c) Third-order SSP Runge-Kutta method



(d) Heun's third-order method



(e) Classic fourth-order Runge-Kutta method

Fig. 2: Convergence error of the Runge-Kutta BUG integrator for the Lyapunov equation with $\theta = 10^{-5}$

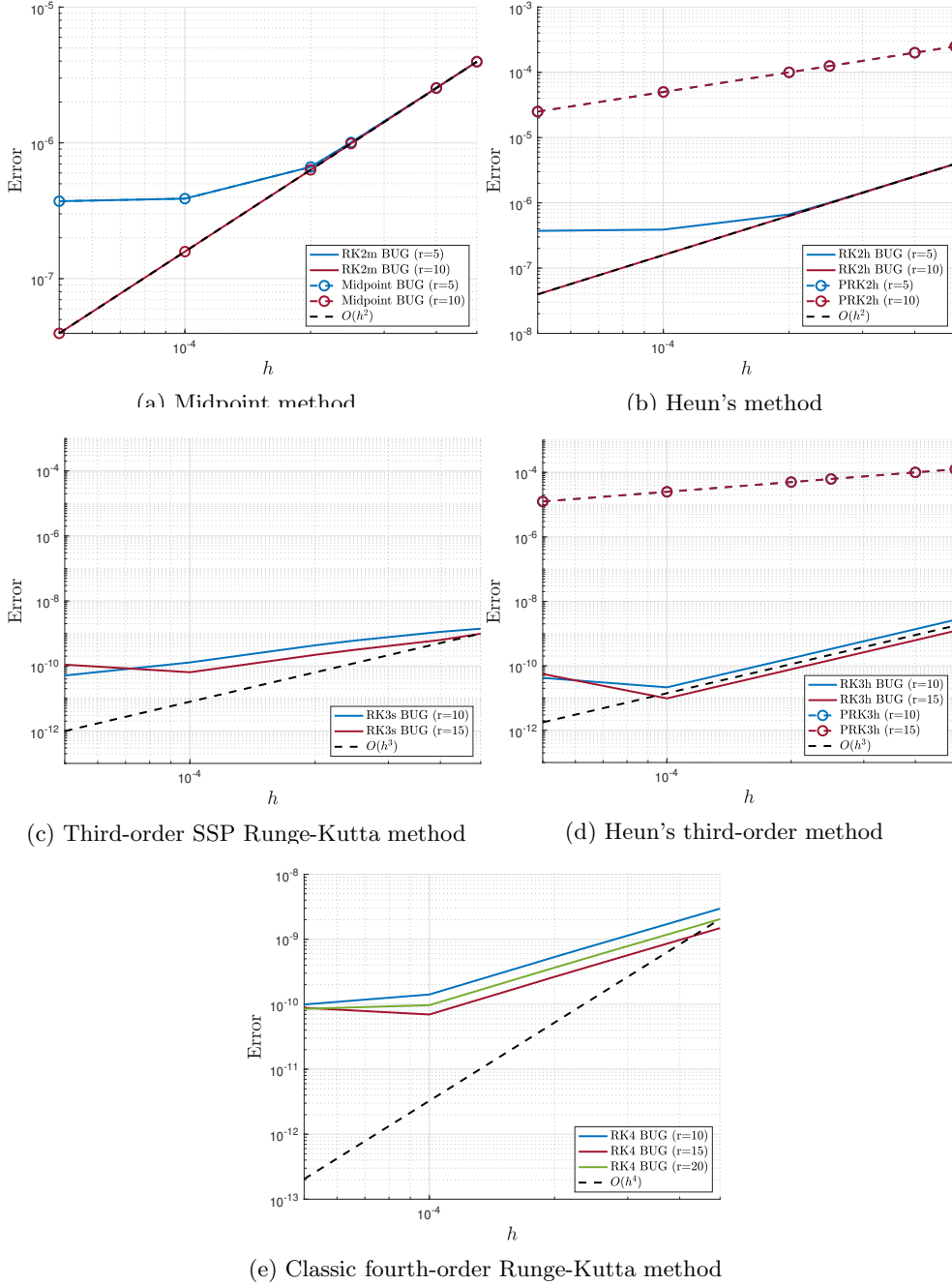


Fig. 3: Convergence error of the Runge-Kutta BUG integrator for the Lyapunov equation with $\theta = 1$. In 3b and 3d, the lines corresponding to the two projected Runge-Kutta methods are superposed as the error is dominated by the low-rank approximation error

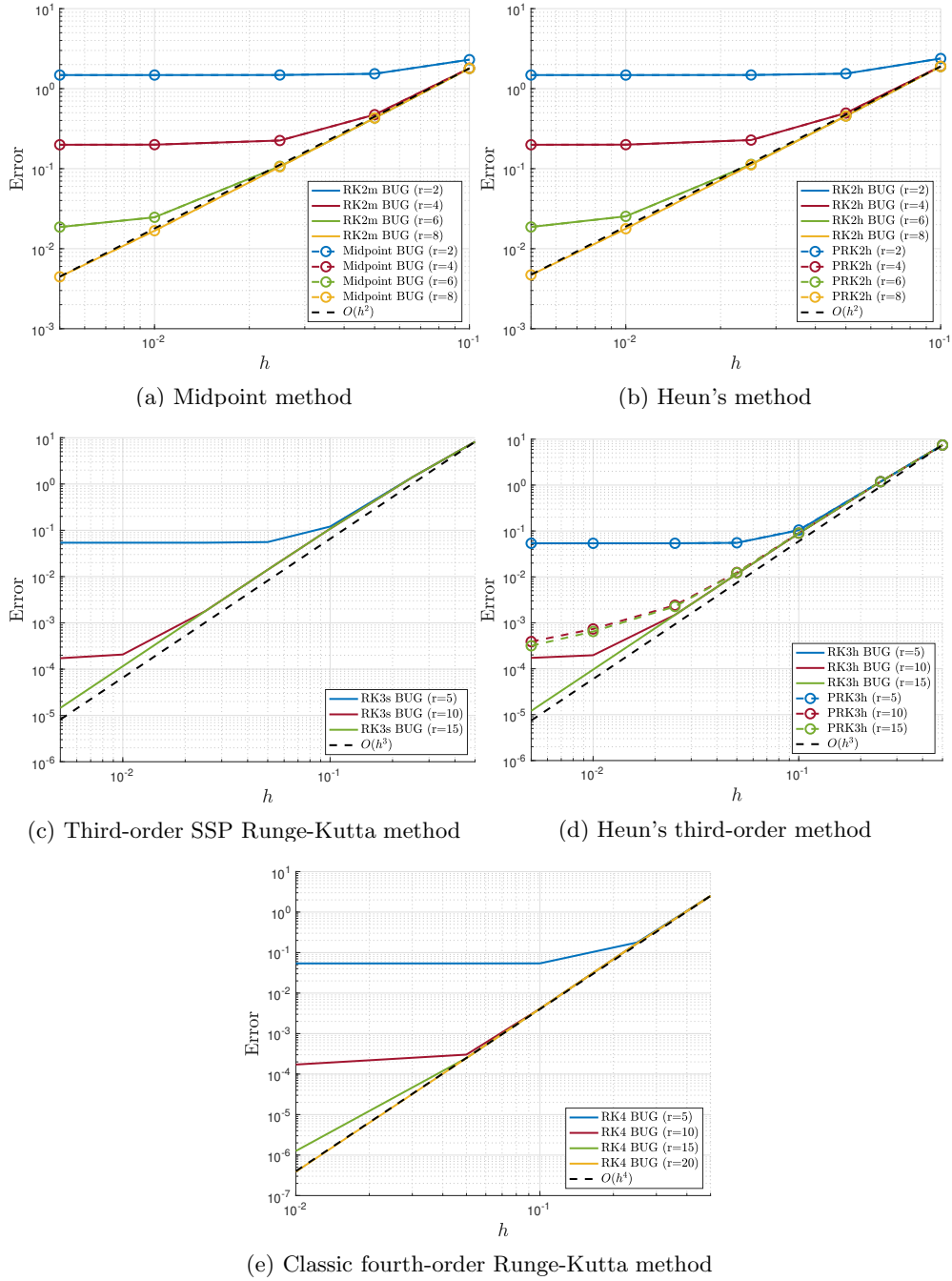


Fig. 4: Convergence error of the Runge-Kutta BUG integrator for the Schrödinger equation with $\theta = 0.1$

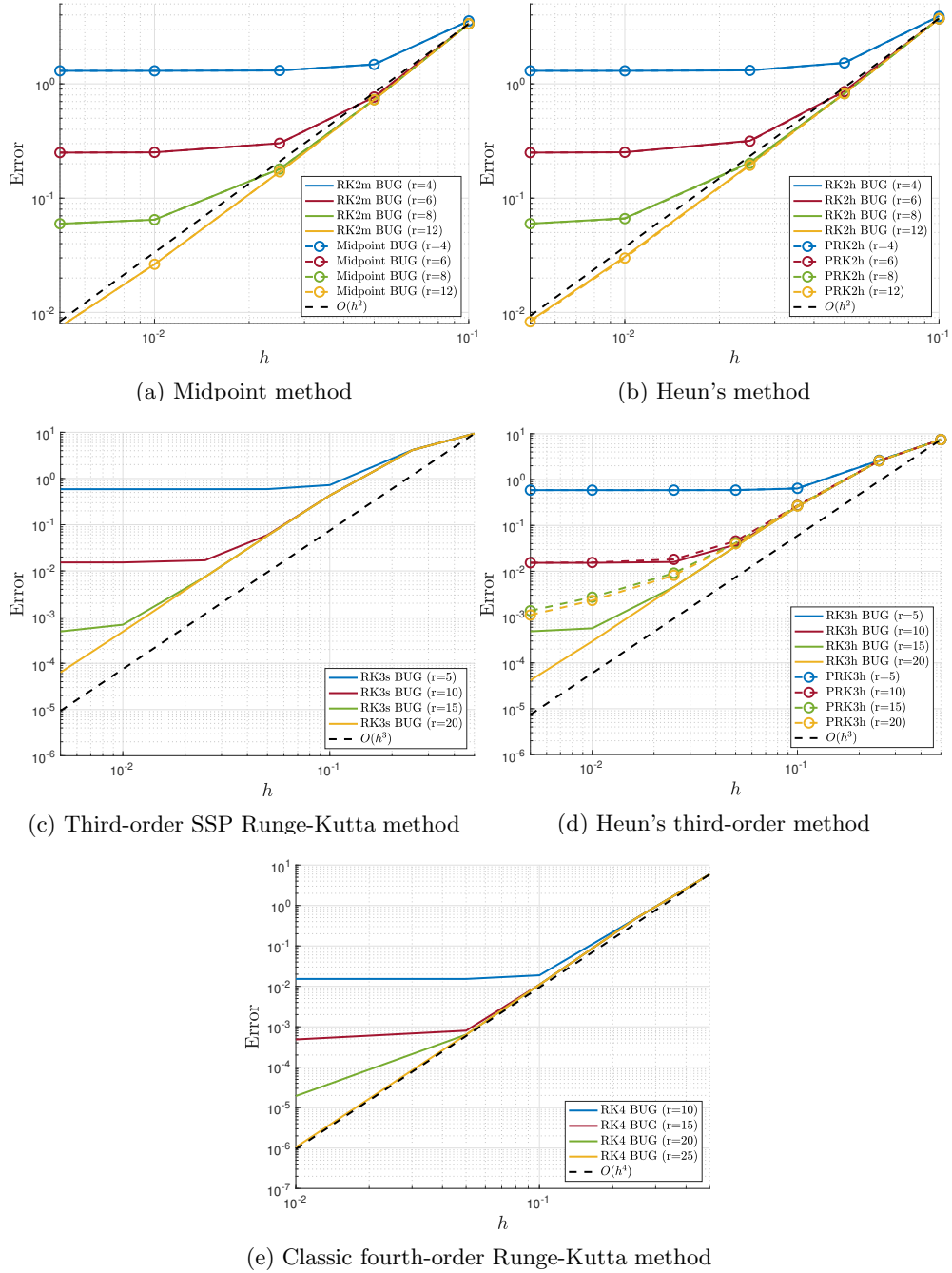


Fig. 5: Convergence error of the Runge-Kutta BUG integrator for the Schrödinger equation with $\theta = 0.3$

numerical test cases. The results demonstrate the high-order convergence of the Runge-Kutta BUG integrator and its superior accuracy compared to projected Runge-Kutta methods for high orders $p \geq 3$ and small time-steps. In perspective, the Runge-Kutta BUG integrator can be extended to other classes of Runge-Kutta methods, such as exponential Runge-Kutta methods or implicit Runge-Kutta methods. These topics will be addressed in future work.

Acknowledgements. This work has been supported by the Swiss National Science Foundation under the Project n°200518 "Dynamical low rank methods for uncertainty quantification and data assimilation".

Declarations

Data availability. The datasets generated during and/or analyzed during the current study are available from the corresponding author on reasonable request.

Conflict of interest. The authors declare that they have no conflict of interest.

Appendix A List of Runge-Kutta methods

The Butcher tableaux associated with the Runge-Kutta methods used in this work are listed below.

- Forward Euler method

$$\begin{array}{c|c} 0 & 0 \\ 1 & 1 \\ \hline & 1 \end{array}$$

- Explicit midpoint method

$$\begin{array}{c|cc} 0 & 0 & 0 \\ 1/2 & 1/2 & 0 \\ \hline & 0 & 1 \end{array}$$

- Heun's method

$$\begin{array}{c|cc} 0 & 0 & 0 \\ 1 & 1 & 0 \\ \hline & 1/2 & 1/2 \end{array}$$

- Third-order SSP Runge-Kutta method

$$\begin{array}{c|ccc} 0 & 0 & 0 & 0 \\ 1 & 1 & 0 & 0 \\ 1/2 & 1/4 & 1/4 & 0 \\ \hline & 1/6 & 1/6 & 2/3 \end{array}$$

- Heun's third-order method

$$\begin{array}{c|ccc} 0 & 0 & 0 & 0 \\ 1/3 & 1/3 & 0 & 0 \\ 2/3 & 0 & 2/3 & 0 \\ \hline & 1/4 & 0 & 3/4 \end{array}$$

- Classic fourth-order Runge-Kutta method

0	0	0	0	0
1/2	1/2	0	0	0
1/2	0	1/2	0	0
1	0	0	1	0
	1/6	1/3	1/3	1/6

References

- [1] Ceruti, G., Kusch, J., Lubich, C.: A rank-adaptive robust integrator for dynamical low-rank approximation. *BIT Numerical Mathematics* **62**(4), 1149–1174 (2022)
- [2] Bernard, F., Iollo, A., Riffaud, S.: Reduced-order model for the BGK equation based on POD and optimal transport. *Journal of Computational Physics* **373**, 545–570 (2018)
- [3] Einkemmer, L., Lubich, C.: A low-rank projector-splitting integrator for the Vlasov–Poisson equation. *SIAM Journal on Scientific Computing* **40**(5), 1330–1360 (2018)
- [4] Einkemmer, L., Ostermann, A., Piazzola, C.: A low-rank projector-splitting integrator for the Vlasov–Maxwell equations with divergence correction. *Journal of Computational Physics* **403**, 109063 (2020)
- [5] Einkemmer, L., Joseph, I.: A mass, momentum, and energy conservative dynamical low-rank scheme for the Vlasov equation. *Journal of Computational Physics* **443**, 110495 (2021)
- [6] Coughlin, J., Hu, J.: Efficient dynamical low-rank approximation for the Vlasov–Ampere–Fokker–Planck system. *Journal of Computational Physics* **470**, 111590 (2022)
- [7] Einkemmer, L.: Accelerating the simulation of kinetic shear Alfvén waves with a dynamical low-rank approximation. *Journal of Computational Physics* **501**, 112757 (2024)
- [8] Einkemmer, L., Kormann, K., Kusch, J., McClarren, R.G., Qiu, J.-M.: A review of low-rank methods for time-dependent kinetic simulations. *arXiv preprint arXiv:2412.05912* (2024)
- [9] Sapsis, T.P., Lermusiaux, P.F.: Dynamically orthogonal field equations for continuous stochastic dynamical systems. *Physica D: Nonlinear Phenomena* **238**(23–24), 2347–2360 (2009)
- [10] Babae, H., Choi, M., Sapsis, T.P., Karniadakis, G.E.: A robust bi-orthogonal/dynamically-orthogonal method using the covariance pseudo-inverse

- with application to stochastic flow problems. *Journal of Computational Physics* **344**, 303–319 (2017)
- [11] Musharbash, E., Nobile, F.: Dual dynamically orthogonal approximation of incompressible Navier Stokes equations with random boundary conditions. *Journal of Computational Physics* **354**, 135–162 (2018)
- [12] Feppon, F., Lermusiaux, P.F.: Dynamically orthogonal numerical schemes for efficient stochastic advection and Lagrangian transport. *Siam Review* **60**(3), 595–625 (2018)
- [13] Musharbash, E., Nobile, F., Vidličková, E.: Symplectic dynamical low rank approximation of wave equations with random parameters. *BIT Numerical Mathematics* **60**(4), 1153–1201 (2020)
- [14] Patil, P., Babae, H.: Real-time reduced-order modeling of stochastic partial differential equations via time-dependent subspaces. *Journal of Computational Physics* **415**, 109511 (2020)
- [15] Kazashi, Y., Nobile, F.: Existence of dynamical low rank approximations for random semi-linear evolutionary equations on the maximal interval. *Stochastics and Partial Differential Equations: Analysis and Computations* **9**(3), 603–629 (2021)
- [16] Kazashi, Y., Nobile, F., Vidličková, E.: Stability properties of a projector-splitting scheme for dynamical low rank approximation of random parabolic equations. *Numerische Mathematik* **149**, 973–1024 (2021)
- [17] Kazashi, Y., Nobile, F., Zoccolan, F.: Dynamical low-rank approximation for stochastic differential equations. *Mathematics of Computation* **94**(353), 1335–1375 (2025)
- [18] Kressner, D., Tobler, C.: Low-rank tensor Krylov subspace methods for parametrized linear systems. *SIAM Journal on Matrix Analysis and Applications* **32**(4), 1288–1316 (2011)
- [19] Weinhandl, R., Benner, P., Richter, T.: Linear Low-Rank Parameter-Dependent Fluid-Structure Interaction Discretization in 2D. *PAMM* **18**(1), 201800178 (2018)
- [20] Benner, P., Richter, T., Weinhandl, R.: A low-rank method for parameter-dependent fluid-structure interaction discretizations with hyperelasticity. *ZAMM-Journal of Applied Mathematics and Mechanics/Zeitschrift für Angewandte Mathematik und Mechanik* **104**(10), 202300562 (2024)
- [21] Riffaud, S., Fernández, M.A., Lombardi, D.: A Low-Rank Solver for Parameter Estimation and Uncertainty Quantification in Time-Dependent Systems of Partial Differential Equations. *Journal of Scientific Computing* **99**(2), 34 (2024)

- [22] Koch, O., Lubich, C.: Dynamical low-rank approximation. *SIAM Journal on Matrix Analysis and Applications* **29**(2), 434–454 (2007)
- [23] Lubich, C., Oseledets, I.V.: A projector-splitting integrator for dynamical low-rank approximation. *BIT Numerical Mathematics* **54**(1), 171–188 (2014)
- [24] Kieri, E., Lubich, C., Walach, H.: Discretized dynamical low-rank approximation in the presence of small singular values. *SIAM Journal on Numerical Analysis* **54**(2), 1020–1038 (2016)
- [25] Kusch, J., Einkemmer, L., Ceruti, G.: On the stability of robust dynamical low-rank approximations for hyperbolic problems. *SIAM Journal on Scientific Computing* **45**(1), 1–24 (2023)
- [26] Ceruti, G., Lubich, C.: An unconventional robust integrator for dynamical low-rank approximation. *BIT Numerical Mathematics* **62**(1), 23–44 (2022)
- [27] Ceruti, G., Kusch, J., Lubich, C.: A parallel rank-adaptive integrator for dynamical low-rank approximation. *SIAM Journal on Scientific Computing* **46**(3), 205–228 (2024)
- [28] Kieri, E., Vandereycken, B.: Projection methods for dynamical low-rank approximation of high-dimensional problems. *Computational Methods in Applied Mathematics* **19**(1), 73–92 (2019)
- [29] Carrel, B., Vandereycken, B.: Projected exponential methods for stiff dynamical low-rank approximation problems. *arXiv preprint arXiv:2312.00172* (2023)
- [30] Ceruti, G., Einkemmer, L., Kusch, J., Lubich, C.: A robust second-order low-rank BUG integrator based on the midpoint rule. *BIT Numerical Mathematics* **64**(3), 30 (2024)
- [31] Kusch, J.: Second-order robust parallel integrators for dynamical low-rank approximation. *arXiv preprint arXiv:2403.02834* (2024)
- [32] Einkemmer, L., Kusch, J., Schotthöfer, S.: Conservation properties of the augmented basis update & Galerkin integrator for kinetic problems. *arXiv preprint arXiv:2311.06399* (2023)
- [33] Harrier, E., Nørsett, S., Wanner, G.: *Solving Ordinary Differential Equations I: Nonstiff Problems*. Springer, Berlin (1993)
- [34] Eckart, C., Young, G.: The approximation of one matrix by another of lower rank. *Psychometrika* **1**(3), 211–218 (1936)
- [35] Horn, R.A., Johnson, C.R.: *Topics in Matrix Analysis*. Cambridge university press, Cambridge (1994)

- [36] Lam, H.Y., Ceruti, G., Kressner, D.: Randomized low-rank Runge-Kutta methods. arXiv preprint arXiv:2409.06384 (2024)
- [37] Trombettoni, A., Smerzi, A.: Discrete solitons and breathers with dilute bose-einstein condensates. *Physical Review Letters* **86**(11), 2353 (2001)